Applied Energy 236 (2019) 318–339

Contents lists available at ScienceDirect

Applied Energy

journal homepage: www.elsevier.com/locate/apenergy

Economic and environmental potential for solar assisted central heating plants in the EU residential sector: Contribution to the 2030 climate and energy EU agenda

Victor Tulus[a], Mohamed Hany Abokersh[b], Luisa F. Cabeza[c], Manel Vallès[b], Laureano Jiménez[a], Dieter Boer[b,*]

[a] Departament d'Enginyeria Química, Universitat Rovira i Virgili, Av. Països Catalans 26, 43007 Tarragona, Spain
[b] Departament d'Enginyeria Mecànica, Universitat Rovira i Virgili, Av. Països Catalans 26, 43007 Tarragona, Spain
[c] GREiA Research Group, INSPIRES Research Centre, Universitat de Lleida, Pere de Cabrera s/n, 25001 Lleida, Spain

HIGHLIGHTS

- The economic and environmental impact of solar district heating systems is studied.
- Multi-objective optimization is carried out in a wide range of EU climate zones.
- A solar fraction above 90% can be achieved for all proposed EU climate zones.
- High environmental performance is realized in solar district heating systems.
- The future fuel prices growth supports the solar district heating economically.

GRAPHICAL ABSTRACT

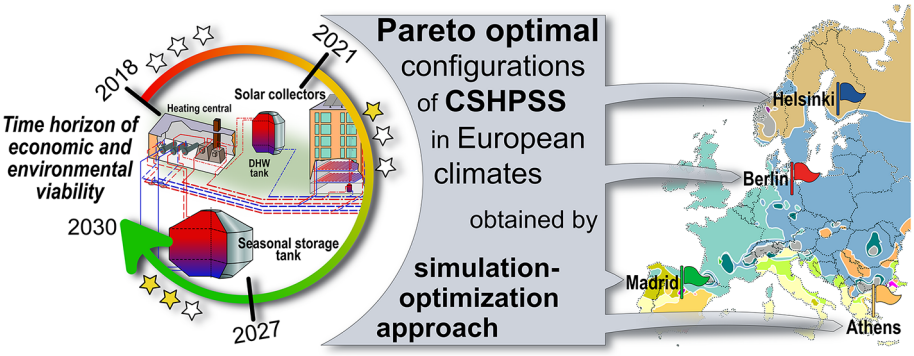

ARTICLE INFO

Keywords:
Central solar heating plant with seasonal storage
Solar community
Life cycle assessment (LCA)
Life cycle cost (LCC)
Multi-objective optimization
2030 climate and energy EU targets

ABSTRACT

Aligning with the ambitious EU 2030 climate and energy package for cutting the greenhouse emissions and replacing conventional heat sources through the presence of renewable energy share inside efficient district heating fields, central solar heating plants coupled with seasonal storage (CSHPSS) can have a viable contribution to this goal. However, the technical performance variation combined with inadequate financial assessment and insufficient environmental impact data associated with the deployment of those innovative district heating systems represents a big challenge for the broad implementation of CSHPSS in Europe. In this context, our paper presents a comprehensive evaluation for the possibility of integrating CSHPSS in the residential sector in various EU member states through the formulation of a multi-objective optimization framework. This framework comprises the life cycle cost analysis for the economic evaluation and the life cycle assessment for the environmental impact estimation simultaneously. The technical performance is also considered by satisfying both the space heating demand and the domestic hot water services. The methodological framework is applied to a residential neighborhood community of 1120 apartments in various EU climate zones with Madrid, Athens, Berlin, and Helsinki acting as a proxy for the Mediterranean continental, Mediterranean, central European, and Nordic climates, respectively. The optimization results regarding the energy performance show that the CSHPSS can achieve a renewable energy fraction above 90% for the investigated climate zones. At the same time, the

* Corresponding author.
E-mail addresses: victor.tulus@urv.cat (V. Tulus), mohamed.abokersh@urv.cat (M.H. Abokersh), lcabeza@diei.udl.cat (L.F. Cabeza), manel.valles@urv.cat (M. Vallès), laureano.jimenez@urv.cat (L. Jiménez), dieter.boer@urv.cat (D. Boer).

https://doi.org/10.1016/j.apenergy.2018.11.094
Received 8 September 2018; Received in revised form 5 November 2018; Accepted 25 November 2018

environmental assessment shows significant improvement when using the CSHPSS in comparison to a natural gas heating system, in those cases the environmental impact is reduced up to 82.1–86.5%. On the other hand, substantial economic improvement is limited, especially in the Mediterranean climate zone (Athens) due to low heating demands and the prices of the non-renewable resources. There the total economic cost of the CSHPSS plants can increase up to 50.8% compared to a natural gas heating system. However, considering the incremental tendency in natural gas prices all over EU nowadays, the study of future plant costs confirms its favorable long-term economic feasibility.

Nomenclature

A_{COL}	total aperture area of solar collectors (m^2)
$C(x_0)$	production cost of a CSHPSS plant at a reference point (€/MWh)
$C(x_t)$	production cost of a CSHPSS plant at a certain time (€/MWh)
CAP_k	design variable of equipment unit k
C_{AUX}	annual operational cost of auxiliary heaters (€)
C_C	total initial capital cost of a CSHPSS plant (€)
$CEPCI^{year\ A}$	chemical engineering plant cost index in the base year
$CEPCI^{year\ B}$	chemical engineering plant cost index in the installation year
C_M	annual cost of equipment unit k (€)
C_O	total discounted operational cost (€)
C_P	annual operational cost of a pump (€)
c_p	specific heat capacity (kJ/kg·K)
C_R	total discounted replacement cost (€)
d	annual discount rate (%)
DAM_d	indicator result for damage category d
FBM_k	bare module factor of equipment unit k
$f_c(x)$	original objective function [$NPC(x)$ or $RCP(x)$]
$\overline{f}_c(x)$	normalized objective function [$NPC(x)$ or $RCP(x)$]
f_m	maintenance factor
$f^{PN}(x)$	pseudo nadir point
$f^{UT}(x)$	utopia point
i	annual inflation rate (%)
IMP_e	indicator result for endpoint impact category e
LCI_i^{MP}	life cycle inventory of the elementary flow i related to the manufacturing process
LCI_i^{OP}	life cycle inventory of the elementary flow i related to operation activities
LCI_i^{TOT}	total life cycle inventory of the elementary flow i
LCI_i^{TR}	life cycle inventory of the elementary flow i related to transportation
LR	learning rate
$\dot{m}_{DHW}$	mass flow rate of the fluid in the DHW distribution circuit (kg/s)
$\dot{m}_{SH}$	mass flow rate of the recirculated fluid in the SH distribution circuit (kg/s)
M_c	big-M values used in the reformulated optimization model
NPC	net present cost (€/MWh)
PEC_k	purchase cost of equipment unit k (€)
PVF_n	present value factor of a single future cash flow at the beginning of the n^{th} time period (-)
PWF_n	present worth factor of periodic future cash flows (-)
$\dot{Q}_{AUX}$	duty of auxiliary heater (MW)
Q_{DHW}	total energy supplied by a domestic hot water tank (MWh)
$Q_{DHW\ load}$	total domestic hot water heating demand (MWh)
$Q_{SH\ load}$	total space heating demand (MWh)
Q_{SST}	total energy supplied by seasonal storage tank (MWh)
RCP	ReCiPe 2008 aggregated impact factor (Pt/MWh)
SF_{DHW}	annual solar fraction for the DHW distribution circuit (%)
SF_{SH}	annual solar fraction for the SH distribution circuit (%)
V_{DHW}	volume of the domestic hot water tank (m^3)
V_{SST}	volume of the seasonal storage tank (m^3)
$WS(x)$	weighted-sum objective function (-)
x	continuous variables of the simulation model
x_0	capacity at the reference point (MW)
x^L	lower bounds of the continuous variables of the simulation model
x_t	capacity at a certain time (MW)
x^U	upper bounds of the continuous variables of the simulation model
y_c	binary variable used in the reformulated optimization model

Greek symbols

α_{CF}	factor of contingency fees (-)
α_k	purchase cost coefficient of equipment unit k
β_k	purchase cost exponent of equipment unit k (-)
δ_d	normalization factor for damage category d
ΔT_{DHW}	temperature difference between the extracted and replaced water inside the DHWT (°C)
ΔT_L	temperature difference between the exit and entrance of the auxiliary heater (°C)
ΔT_{SST}	temperature difference between the extracted and replaced water inside the SST (°C)
ε_d	weighting factor for damage category d
θ_{ei}	characterization factor that connects the elementary flow i with endpoint impact category e
λ	non-negative weight for the weighted-sum method

Abbreviations

AUX	auxiliary heater fueled by natural gas
COL	field of solar collectors
CSHPSS	central solar heating plant coupled with seasonal storage
DHW	domestic hot water
DHWT	domestic hot water storage tank
GHG	greenhouse gas
GenOpt	generic optimization program
GPSPSOCCHJ	hybrid generalized pattern search with particle swarm optimization with construction coefficient and Hooke-Jeeves algorithms
HE	heat exchanger
HJ	Hooke-Jeeves algorithm
LCA	life cycle assessment
LCC	life cycle costing
MOO	multi-objective optimization
P	centrifugal pump
PSO	particle swarm optimization algorithm
SH	space heating
SST	seasonal storage tank
TES	thermal energy storage
TRNSYS	transient system simulation program

Indices

c	objective function
d	damage category

e	endpoint impact category	*Sets*	
i	elementary factor		
k	equipment unit	ID_d	set of endpoint impact categories e that contribute to damage d

1. Introduction

The global tendency for changing the world energy map is a booming topic, and more efforts should be scaled up to shift the current energy production systems towards the use of cleaner and less carbon-intensive sources. Currently, fossil fuels share about 80% of the primary energy use [1]. The International Energy Outlook [2] forecasts a significant increase in the world energy demand over the next decades. It is projected that global energy consumption will evolve by 48% in 2040 with a growth in the usage of crude oil and natural gas by 30% and 53.2%, respectively. This outlook trend leads to serious environmental problems such as more greenhouse gas (GHG) emissions and the subsequent impact on the climate [3].

Europe is one of the relevant players in this scenario contributing 21.6% to the overall energy consumption [4]. Additionally, in the European Union (EU) the building stock accounts for about 40% of the total energy demand [5], while the residential sector consumes 63% of this energy [6]. According to estimations of the US Energy Information Administration (EIA) [2], the energy consumption demand for the residential section in the EU increases by an average of 0.9% per year. Along with all of these figures, the residential buildings are the fourth most important source of GHG in the EU, and it accounted for about 10% of the total GHG in 2016 [7]. In response to this challenge, the EU has adopted the 2020 climate and energy package [8] which includes requisite legislation to tackle the environmental concerns and support the energy security and independence. The package sets three main targets: (i) reduce by 20% the GHG emissions compared to the 1990 levels, (ii) increase the renewable energy share and (iii) improve its energy efficiency by 20%. In 2013, the EU approved a new ambitious framework for the climate and energy between 2020 and 2030. This strategy plans to cut the GHG emissions by 40%, to achieve a share of at least 27% of renewable energies, and to improve the energy efficiency by at least 27% [9].

Among all of the renewable energy resources, the solar thermal energy obtained considerable attention since it is a CO_2 neutral and it can be used for both space and water heating [10,11]. It was reported that solar thermal technologies could substantially satisfy the heat demand in the residential sector in many countries [12]. Furthermore, it has several advantages which include [13] (i) savings in the primary energy consumption at the end user and country planning level, (ii) increase in energy security against the fluctuations in the prices of the conventional energy resources, (iii) decrease the dependency on the electricity from the network, and (iv) contribute to the network stabilization. These solar thermal energy systems continue to increase their market share across whole Europe. More than 1.2 $GW_{thermal}$ was installed within 2015 to raise the total installed capacity to 34.4 $GW_{thermal}$ [14].

However, the solar thermal systems are facing a significant challenge of intermittency and predictability, which cause a gap between the supply and the energy demand [15,16]. The thermal energy storage (TES) systems can effectively solve this issue [17]. There are three main categories of the TES. These categories include the sensible TES through a temperature gradient, the latent TES based on the phase change materials, and the thermo-chemical TES through chemical reactions [18]. Currently, sensible storage is the most common system to be used in the residential sector, while latent and chemical systems are promising technologies under development [19].

The specific heat and energy density are the two main characteristics that evaluate the thermal capacity of the sensible TES. Besides thermal capacity characteristics, the TES cost also has a vital role in the selection process. Therefore, water, rock material, and soil/ground are the usually employed storage media in sensible TES systems. The energy storage in the sensible TES systems can be classified into long-term (seasonal) and short-term (diurnal) [20]. The main difference between these two systems is the solar collector and storage volume sizing where the investment per square meter of collector area is almost doubled in the long-term seasonal storage systems [21]. In addition to that, seasonal storage is always coupled with an auxiliary heater to cover the shortage in supply [22]. On the contrary, short-term storage allows direct usage in the heating district network.

The solar district heating system coupled with sensible seasonal storage has been subjected to several investigations, and it has already been introduced as a feasible alternative. Initially, in the 1950s, Speyer [23] assesses theoretically the potential of the central solar heating plant coupled with seasonal storage (CSHPSS) to benefit from the excess of solar energy in summer during the winter period. The first proof of concept for this system was developed in Sweden in the 1970s to address the energy shortage crisis [24], followed by Denmark and Germany in the 1990s [25]. Since then, the market for solar heating plants has grown throughout Europe [26], particularly in Northern and Central European countries. During 2016, 37 large heating plants were installed in Europe compared to 21 new installed in 2015. Within these installations, 31 systems were added to the Denmark district heating networks, four systems in Germany, one system in Sweden and one system in France [27]. In the southern European countries, some positive signs of growth of solar thermal energy are noticed from Spain and Greece. These evolution signs are due to the legislation imposed by the governments to scale up the utilization of renewable energy technologies [28].

Several research entities such as the IEA's Task 32 and Task 45 [29] has paid attention to the solar district heating energy systems. Additionally, numerous articles discuss the principal methods available for the seasonal storage of the central solar heating system. Xu et al. [30] and Rad and Fung [31] presented an extensive review on the solar district energy system and its different types of TES. Shah et al. [32] conducted a comparative review to demonstrate the potential contribution of different TES options with a goal of building a decision support flowchart for the selection of TES based on the required application. In this context, Sibbitt et al. [33] and Antoniadis and Martinopoulos [19] developed several useful guidelines for the design of the CSHPSS. Rehman et al. [34], and Rämä and Mohammadi [35] conducted investigations toward the different options for community-sized solar thermal storage system configurations for the Nordic European climate zones. Also, Rad et al. [36], and Panno et al. [37] assessed the techno-economic promising performance of the seasonal solar thermal storage in the residential sector. Finally, Ciampi et al. [38] demonstrated its environmental potentials.

In order to maximize the benefits from the centralized solar heating plants with seasonal storage in the residential sector, the optimal sizing of the system components and their operation should be adequately planned. This process can turn into a computationally requesting task. Li et al. [39] explored the optimal operation strategy for the CSHPSS based on the orthogonal schedule using real data. Durão et al. [40] and Rehman et al. [41] lean towards optimizing the design parameters of CSHPSS for different locations from an economical point of view using Genetic Algorithms, whereas Hirvonen et al. [42] also consider the community size effect. Buoro et al. [43] formulated a Mixed Integer Linear Programming (MILP) approach for optimizing the CSHPSS plant

together with a conventional power unit for a large district heating network. Recently, several studies emphasized on the importance of taking into account the techno-economic parameters and the environmental impact simultaneously which expands the optimization approach for designing a new CSHPSS plant from a single objective optimization to a multi-objective optimization (MOO) problem. Tulus et al. [44] proposed a systematic MOO approach for designing CSHPSS plants based on a generic optimization tool according to economic and environmental indicators. The optimization of the environmental indicators become especially important as the main impact weight shifts from the fossil fuel consumption to the materials used for the installation of the system. Equally, Pavičević et al. [45] demonstrated a long-term MILP optimization model based on SCIP (Solving Constraint Integer Program) solver for district heating systems. This model is capable of handling the operation strategy and system component sizing in the planning and evaluation process with considerations for the cost and the environmental impacts throughout the project lifetime. In addition, Welsch et al. [46] proposed an MOO approach for investigating solar district heating systems under various economic and environmental boundary conditions. Projection of the results promotes the influence of CSHPSS in increasing the feasibility of renewable energy technologies in the building sector.

Even though the tendency of the CSHPSS plants is promising, a range of potential barriers (technical, financial and administrative) are still obstructing the wide deployment of CSHPSS in Europe. One of the most important challenges associated with the CSHPSS is the significant performance variations. According to several large-scale seasonal energy storage systems, the solar fraction of the plants has a quite wide variation [47] which suggests a high degree of variation in the quantifiable costs and benefits. In German and Spanish CSHPSS projects [31,36] the combination of seasonal heat storage with a central solar heating system enables solar fractions of over 50%. While in a CSHPSS project for a residential area in Alberta (Canada) 97% of solar fraction was achieved in the fifth year of operation [33]. A simulation study for district solar heating combined with seasonal borehole storage in Helsinki showed that high solar fraction of 96% is feasible [48]. Besides the performance variation, the high capital costs of this technology represent a challengeable barrier and make it more difficult to obtain the required funding [49,50]. Also, there are primarily political and legal barriers which include: lack of a standardized model of the system which could help the European 2030 climate and energy framework achieve its targets; the sudden change in the renewable energy legal framework in some EU countries such as Spain [51]. All these technical, economic and legal barriers promote high variation in quantifying the CSHPSS benefits over its lifetime and add more difficulties for the EU members to state their forecast plans for future deployment of the CSHPSS in district heating fields.

Aligning with the challenges facing the wide deployment of CSHPSS in Europe combined with the ambitious EU 2030 climate and energy package for cutting the greenhouse emissions and increasing the share of renewable energies. The potential evaluation of a refurbished or a new solar district heating system requires not only its technical specification but its potential contribution when integrated into the end-user supply network taking into account the renewable source availability during various seasons of the year and the weather and ground conditions [52]. Thus, such issues call for developing an adaptive methodological framework to the local weather conditions [53].

Due to the complexity of the CSHPSS design and its inconsistencies in the energy production combined with the challenges associated with its economic and environmental impact. The novelty in this work is to develop a methodological framework that supports the climate and energy goals of the EU through a comprehensive analysis for the techno-economic advantages and environmental impacts of CSHPSS plants in various EU member states with a comparison to a conventional heating system using natural gas as the primary heat source. In this context, a simulation-optimization methodology is developed with a detailed simulation of the CSHPSS plant performance using TRNSYS 18 software [54] considering seasonal and short-term storage systems and their respective load profiles based on the explored climates. Then a multi-objective optimization is performed by an external generic optimization toolbox (GenOpt [55]). The proposed methodology can serve as a supportive tool for decision-makers helping them assess the potential of the CSHPSS plants in Europe and subsequently, promote a clear statement towards the possibility of achieving the 2030 European climate and energy framework targets.

The article organization is the following: in Section 2 a general overview of the CSHPSS system is provided. The mathematical formulation of the simulation-optimization methodology together with the mathematical basis of the CSHPSS market forecasting is provided in Section 3. Section 4 describes the application of the methodology to four EU climate zones, and Section 5 offers the necessary results and discussions. Finally, the conclusions of the work are presented in Section 6.

2. Overview of the CSHPSS system

Central solar heating plants with seasonal thermal energy storage are designed to fulfill energy demands for space heating (SH) and domestic hot water (DHW) in a residential sector (see Fig. 1). Usually, these systems are designed to supply district heating for more than 100 apartments with a solar fraction of approximately 50% [56]. The main components of the CSHPSS system are the thermal solar collector, the seasonal storage tank (SST), and the DHW storage tank (DHWT). The solar collector transfers the heat gained from the solar radiation to the storage tanks which is then supplied to the customer on demand. The mismatching between the energy supply and demand in the daily and seasonal bases is balanced through the storage tanks. Auxiliary natural gas heaters are installed to back up the required heat demand in case the solar heating system failed to cover it.

The SST facilitates long-term storage of thermal energy used to cover the SH demand during a winter season with solar energy stored during a summer period. The long-term storage implies relatively large dimensions for the SST which favors slow charging and discharging processes. On the other hand, the DHWT is a short-term independent storage tank which is used to cover the daily DHW service at a temperature of 60 °C.

The proposed CSHPSS system is divided into four circuits, three of them are closed: solar field circuit, seasonal storage circuit, and SH distribution circuit; and the last one, DHW distribution circuit, is open (*i.e.*, fed from the water main) as shown in Fig. 2. The water-glycol mixture is the primary heat transfer fluid in the solar field circuit. The solar energy is collected through the field of solar collectors (COL), and a centrifugal pump (P_1) impulses the fluid to reach the heat exchangers (HE_1) and (HE_2). These heat exchangers connect the solar field circuit to the seasonal storage circuit or DHW distribution circuit depending on the selected control mode through Y-type valves. The heat exchangers separate the solar field circuit from the SST and DHWT to protect the solar collectors from damage [57].

In the DWH operation mode (priority 1) the monitored variables are the average DHWT temperature and the COL output temperature. Once the mode is triggered, the centrifugal pumps P_1 and P_4 are activated, and the water is sent towards the DHWT through HE_2. A natural gas boiler AUX_2 is installed to cover any occasional shortages in the thermal energy supply to the DHW network. Two Y-type valves regulate the water temperature which arrives at the DHW network through the mixing of fresh water from the water main with the hot water coming from the AUX_2.

In the SH operation mode (priority 2) the monitored variables are the SST temperatures, the average DHWT temperature, and the COL output temperature. Once the average DHWT temperature hits its set-point and the COL output temperature is higher than the SST bottom temperature, the mode is activated by starting pumps P_1 and P_2 and

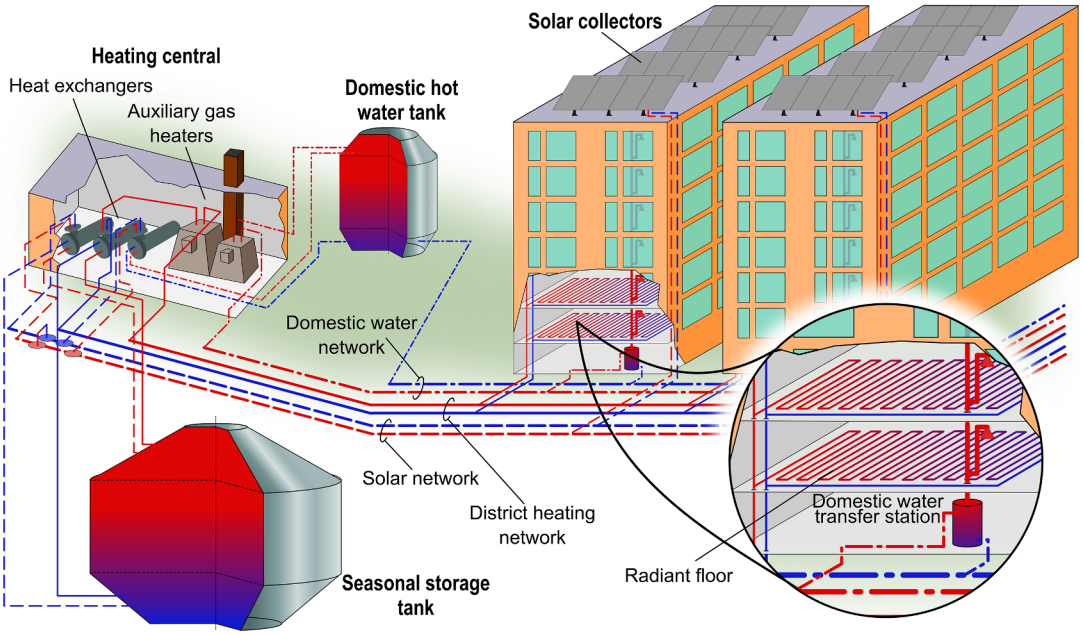

Fig. 1. Overview of the central solar heating system with long and short-term storage tanks coupled to a district heating network.

allowing the heat transfer through HE_1 in order to charge the SST. During the heat demand period, a variable speed pump P_3 impulses the cold water to the bottom of the SST and discharges the hot water to the HE_3 that connects the seasonal storage circuit to the SH distribution circuit. Downstream the HE_3 a natural gas boiler AUX_1 is installed. This boiler operates when the SST cannot reach the setpoint. The combination of two Y-type valves regulates the water temperature arriving at the heating network through back-mixing of the returned water from the network with the hot water coming from the AUX_1.

Beside these two operation modes, the simultaneous SH and DWH mode (priority 3) is also established and regulated based on the controlling system when the conditions of the two previous modes are satisfied.

Additional control loops regulate the operation of the Y-type valves in the SH and DHW distribution circuits in order to maintain the established setpoints at the entrances of the heating and DHW networks.

3. Methodological framework

Our simulation-optimization approach [58–60] incorporates the evaluation of a CSHPSS plant performance at various EU locations and the definition of a set of optimal configurations of the plant from both techno-economic and environmental aspects simultaneously. Thus, the proposed methodology is a multi-objective optimization problem. The transient performance of the CSHPSS plant is modeled in TRNSYS 18, simulation software which allows interconnecting available standard equipment units to obtain more complex systems. The optimization is performed externally using a generic optimization toolbox, GenOpt.

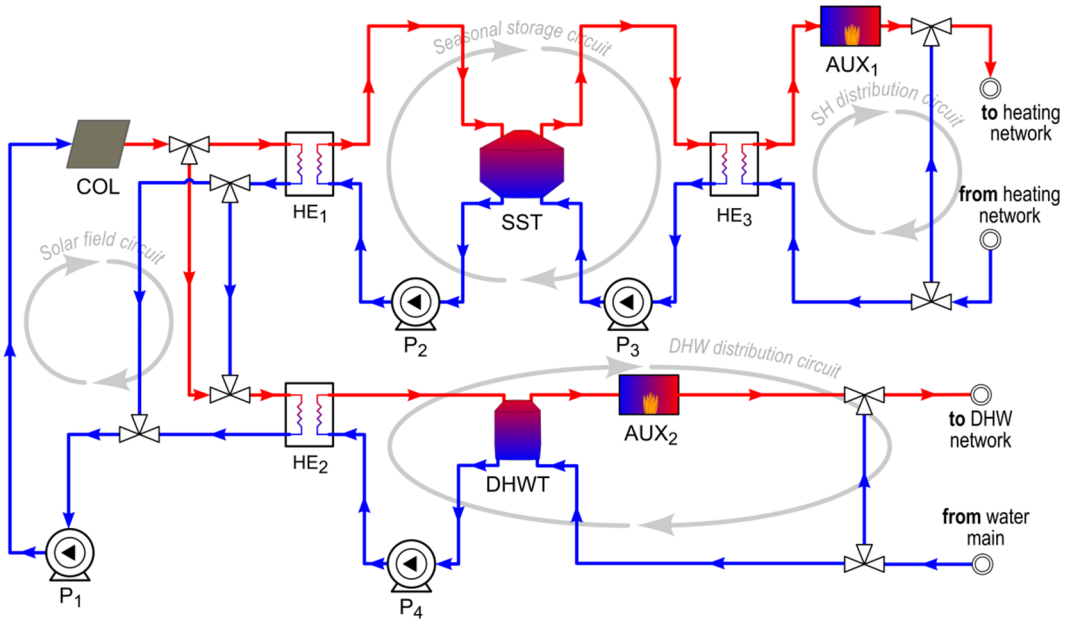

Fig. 2. Process flow diagram of the CSHPSS plant simulated in TRNSYS 18, where COL is the field of solar collectors, SST is the seasonal storage tank, DHWT is the domestic hot water tank, AUX_i are the auxiliary heaters, HE_i are the heat exchangers, and P_i are the centrifugal pumps.

The first subsection of the methodology illustrates the developed TRNSYS model and its input and output data. The second subsection shows the techno-economic and environmental criteria for assessing the proposed CSHPSS. Finally, the third subsection dives deeper into the optimization framework itself and the implemented algorithm.

3.1. TRNSYS simulation model

TRNSYS 18, transient simulation software, is employed to analyze the dynamic behavior of the proposed CSHPSS. The software operates by solving partial differential equations of the mass and energy balances within previously defined boundaries.

The dynamic nature of the program intends to offer a realistic simulation of the CSHPSS plant. On the other hand, to reduce the computational cost, the model is simulated over a typical year of operation, and the solution is extrapolated over the plant lifetime assuming same climatic conditions and demand profiles year after year.

The proposed simulation model follows the models previously developed by Guadalfajara et al. [61] and Tulus et al. [44] with modifications to include the DHW distribution circuit and a more sophisticated controlling loop. See the information flow diagram presented in Fig. 3 for details about the individual components (called Types inside the software) used in TRNSYS. Each type has three main information boxes which include the component-specific parameters, input variables, and output variables.

The main types used in our CSHPSS model are: flat plate solar collectors (Type 1a) with an optical efficiency of 0.817, heat loss coefficient of 2.205 W/m^2·K; sensible storage tanks (Type 4c) with heat loss coefficient of 0.06 W/m^2·K and 0.3125 W/m^2·K for the SST and DHWT, respectively; counterflow heat exchangers (Type 5b) with overall heat transfer coefficient of 3931 W/m^2·K; and auxiliary heaters (Type 6) with an efficiency of 93%. The secondary model types are: single speed centrifugal pumps (Type 3b), inlet and outlet pipe ducts (Type 709), three-way valves (Type 11 h), controlled flow diverters (Type 11f), tempering valves (Type 11b), soil temperature profile for the SST (Type 77), weather data processor (Type 15-3), time-dependent forcing functions for the heating and DHW demand profiles (Type 9c), and controllers (Type 2b).

3.2. Evaluation criteria

Several evaluation criteria were formulated in order to quantify the CSHPSS performance.

3.2.1. Technical criteria

The technical evaluation of the dynamic behavior of the CSHPSS plant is described through several parameters that include the energy supplied by the SST, DHWT, and auxiliary boilers.

The storage tank has a vital role in the CSHPSS plant performance. Thus, the energy provided by the fully stratified seasonal and DHW storage tanks are described in Eqs. (1) and (2), respectively [62]:

$$Q_{SST} = \int_0^t \dot{m}_{SH}\, c_p \Delta T_{SST} \tag{1}$$

$$Q_{DHW} = \int_0^t \dot{m}_{DHW}\, c_p \Delta T_{DHW} \tag{2}$$

where $\dot{m}_{SH}$ and $\dot{m}_{DHW}$ are the mass flow rates of the recirculated water inside the SH and the DHW distribution circuits, respectively, c_p is the specific heat capacity, ΔT_{SST} and ΔT_{DHW} are the temperature differences between the extracted and replaced water at storage tanks to cover the SH and DHW load, respectively.

Auxiliary boilers are utilized to cover the SH demand and the DHW demand when the solar system is unable to reach the set temperature point. The auxiliary energy rate supplied to the SH and DHW networks

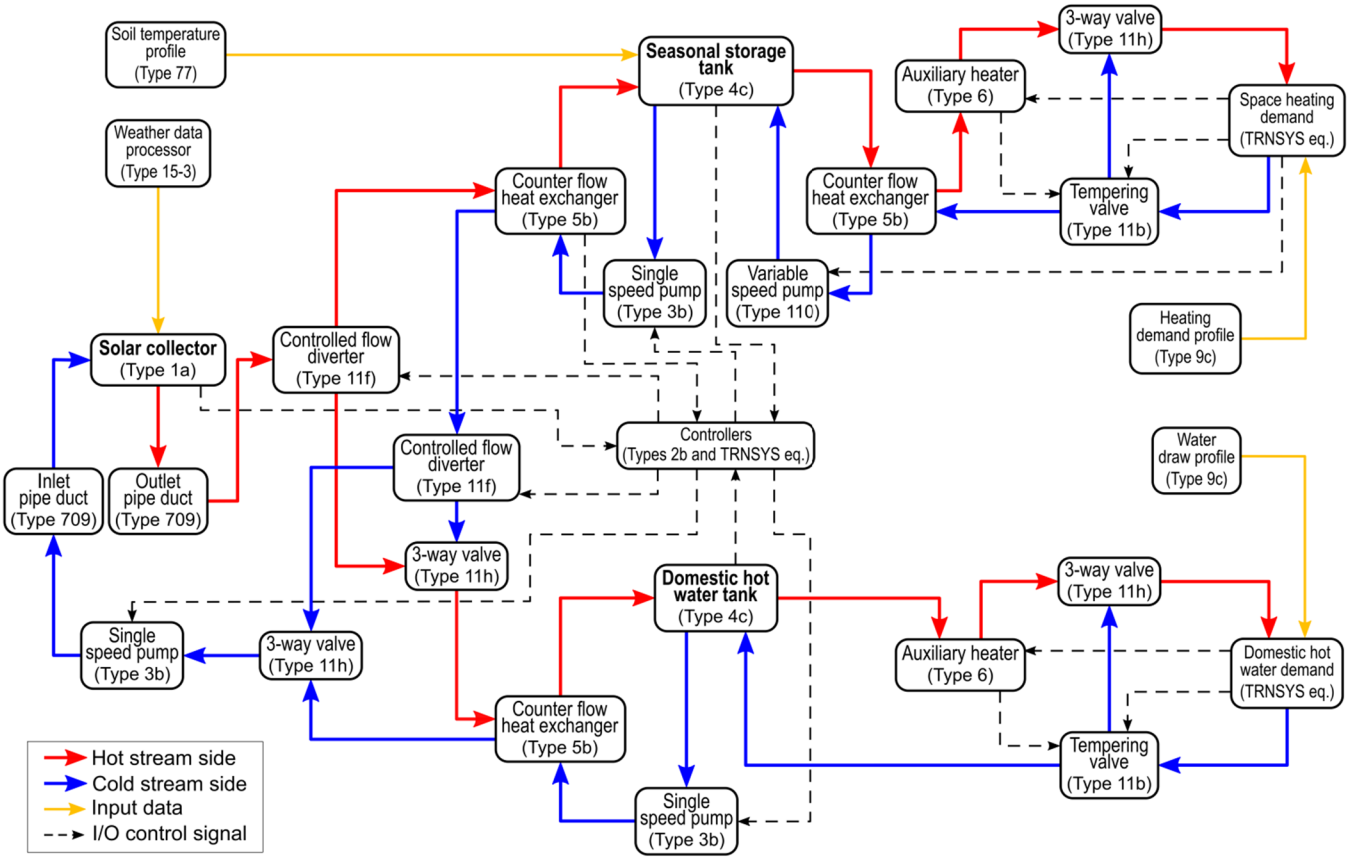

Fig. 3. Information flow diagram of the CSHPSS system modeled in TRNSYS 18 with the representation of the software components and their interconnections.

can be expressed as shown in Eqs. (3) and (4), respectively [63]:

$$\dot{Q}_{AUX1} = \dot{m}_{SH} c_p \Delta T_L \tag{3}$$

$$\dot{Q}_{AUX2} = \dot{m}_{DHW} c_p \Delta T_L \tag{4}$$

where ΔT_L is the temperature difference between the exit and entrance of the auxiliary heater.

Annual solar fraction [64,65] for the SH and DHW distribution circuits are introduced as technical performance indicators. These indicators can be computed using Eqs. (5) and (6) as a function of the heating network demand ($Q_{heating\ load}$), and the DHW network demand ($Q_{DHW\ load}$).

$$SF_{SH} = 1 - \frac{\int_0^t \dot{Q}_{AUX1}}{Q_{\text{heating load}}} \tag{5}$$

$$SF_{DHW} = 1 - \frac{\int_0^t \dot{Q}_{AUX2}}{Q_{\text{DHW load}}} \tag{6}$$

3.2.2. Economic criteria

In the current study, the economic evaluation of the CSHPSS system follows the work of Tulus et al. [44] which is carried out based on the life cycle costing (LCC) methodology [62,66].

The LCC methodology is a valuable monetary approach for assessing the energy system designs in terms of the initial purchase cost and the operational costs throughout the expected lifetime of the system. The LCC perspective in the early stages of design empowers the decision-makers to deeply comprehend the lifetime costs of the system [45], and subsequently enhance the possibility of an additional reduction in the system operational cost even if more investment cost is required [67].

The main principle of the LCC methodology is the future cost approach. Its feature is to discount the summation of all expenses during the lifetime of the system to its present value where the net present cost (*NPC*) can be estimated by adding the initial capital cost (C_C), the operational cost (C_O) and the total replacement cost of the equipment (C_R):

$$NPC = C_C + C_O + C_R \tag{7}$$

3.2.2.1. Initial capital cost. The initial capital cost is the investment cost at the project starting point. It takes into consideration the actual equipment cost, the installation labor, and transportation costs along with any possible contingency expenses:

$$C_C = (1 + \alpha_{CF}) \sum_k (PEC_k \cdot FBM_k) \tag{8}$$

where PEC_k is the initial purchase cost of equipment unit k, FBM_k denotes the bare module factor, which represents the installation labor and transportation costs, and α_{CF} denotes the contingency fees factor.

The PEC_k is brought from the base year (*year A*) to the year of installation (*year B*) using the Chemical Engineering Plant Cost Index (*CEPCI*) [68] as follows:

$$PEC_k = PEC_k^{yearA} \frac{CEPCI^{yearB}}{CEPCI^{yearA}} \qquad \forall\ k \tag{9}$$

The initial purchase cost of equipment unit k at year A can be estimated as shown in Eqs. (10) and (12) [69–72]:

$$PEC_k^{yearA} = \alpha_k CAP_k^{\beta k} \qquad \forall\ k = COL, SST, DHW, AUX \tag{10}$$

$$PEC_k^{yearA} = CAP_k^{\beta k} \cdot 10^{[\alpha_k (\log_{10} CAP_k)^{\beta_k}]} \qquad \forall\ k = HE_1, HE_2 \tag{11}$$

$$PEC_k^{yearA} = \alpha_k \ln\left(\frac{CAP_k}{1000}\right) + \beta_k \qquad \forall\ k = P_1, P_2, P_3, P_4 \tag{12}$$

where α_k and β_k are the equipment purchase parameters of unit k and CAP_k is the design variable of unit k. In the current study, the design variables are the solar collector area (A_{COL}), the volume of the storage tanks (V_{SST}, V_{DHW}), the capacity of the auxiliary heaters (AUX_1, AUX_2), the effective heat transfer area of the heat exchangers (HE_1, HE_2, HE_3) and the mass flow rates of the pumps ($\dot{m}_1$, $\dot{m}_2$, $\dot{m}_3$).

3.2.2.2. Operational cost. The operational cost refers to the sum of all the annual operating costs such as maintenance costs of the different equipment units and facilities, the consumption of electricity by hydraulic equipment and the consumption of natural gas by auxiliary heaters. It can be expressed as follows:

$$C_O = C_M PWF_M + C_P PWF_P + C_{AUX} PWF_{AUX} \tag{13}$$

where C_M, C_P, and C_{AUX} represent the annual maintenance cost, hydraulic equipment (*i.e.*, pumps) and auxiliary consumption costs, respectively. The present worth factor (*PWF*) counts for the time value of money considering the inflation rate (i), the discount rate (d), and the lifetime of the proposed system (N_e) as expressed in Eq. (14):

$$PWF = \begin{cases} \frac{1}{d-i}\left[1 - \left(\frac{1+i}{1-d}\right)^{N_e}\right] & \forall\ i \neq d \\ \frac{N_e}{1+i} & \forall\ i = d \end{cases} \tag{14}$$

3.2.2.3. Replacement cost. Several equipment units in the CSHPSS plant have a high depreciation rate and subsequently, need to be replaced during the plant operation. These units are the field of solar collectors, the heat exchangers, and the auxiliary heaters. The replacement cost can be expressed as shown in Eq. (15) with consideration for the present equipment value:

$$C_R = PVF_n \sum_k (PEC_k \cdot FMB_k) \tag{15}$$

where PVFn is the present value factor of future cash flow at year n, and it can be expressed as follows:

$$PVF_n = \frac{(1+i)^n}{(1+d)^n} \tag{16}$$

3.2.3. Environmental criteria

The LCC is purely based on an economic approach not considering the environmental performance of the CSHPSS plant. In this context, the environmental impact is assessed by using the life cycle assessment (LCA) methodology. This methodology enables a comprehensive estimation of the local environmental impacts by analyzing the product lifecycle from a global perspective. Thus, LCA assesses the product based on the "cradle-to-grave" concept [73] taking into account a range of environmental categories. The LCA methodology was standardized through ISO 14040 series [74–76], and it comprises four main phases which trail a specific sequence: goal and scope definition, inventory analysis, impact assessment, and interpretation. These phases are depicted in details in the next subsections as mentioned previously by Guillén-Gosálbez et al. [77].

3.2.3.1. Goal and scope definition. This phase comprises three main scopes: the system, its boundaries, and the functional unit. In the system boundary, the entire product life cycle should be analyzed ("cradle-to-grave" concept). However, this study focuses on the CSHPSS plant itself, which is connected to an existing district heating network. Therefore, the system boundary would be drawn based on the "cradle-to-gate" concept with exclusion for the end user distribution networks, that is, from the extraction of raw materials for equipment units manufacturing to delivery of hot water to the district heating network. The functional unit in this study is the energy amount demanded by the end user in order to cover his heating and hot water necessities over the entire time horizon.

3.2.3.2. Inventory analysis. Inventory analysis is the second phase in the LCA sequence which quantifies the input and output materials and the energy consumption associated with the CSHPSS plant construction and operation. In the current problem, several sources of impact are considered: equipment manufacturing and utility energy consumption (natural gas and electricity) by the system during the whole lifetime (LCI_i^{MP}); transportation to the site of material and finished equipment units (LCI_i^{TR}); plant operation during the entire time horizon (LCI_i^{OP}).

These resources consumption associated with the whole elementary flows during its lifetime has been retrieved from the Ecoinvent 3.0 database [78]. Mathematically, the inventory entries can be expressed as follows:

$$LCI_i^{TOT} = LCI_i^{MP} + LCI_i^{TR} + LCI_i^{OP} \qquad \forall\, i \tag{17}$$

where LCI_i^{TOT} is the total life cycle inventory associated with the elementary flow i. LCI_i^{MP}, LCI_i^{TR}, and LCI_i^{OP} refer to the manufacturing processes, the transportation tasks and the plant operation associated with the elementary flow i, respectively.

3.2.3.3. Impact assessment. In this phase, the inventory data are translated into environmental impacts. As mentioned previously, three different damage categories include the human health, the ecosystem, and the resources damages based on the ReCiPe 2008 framework [79]. The characterization of the promoted framework has been carried out based on the endpoints level not considering the midpoints. Mathematically, the impact values associated with each impact category can be expressed as follows:

$$IMP_e = \sum_i \theta_{ei} \cdot LCI_i^{TOT} \qquad \forall\, e \tag{18}$$

where θ_{ei} denotes the characterization factor which links the elementary flow i with endpoint impact category e.

Finally, the endpoint impact categories e are aggregated into damage categories (DAM_d), which are further normalized and aggregated into a single final indicator RCP as stated in Eqs. (19) and (20):

$$DAM_d = \sum_{e \in ID_d} IMP_e \qquad \forall\, d \tag{19}$$

$$RCP = \sum_d \delta_d \varepsilon_d DAM_d \qquad \forall\, d \tag{20}$$

where ID_d represents a set of endpoint impacts e that contribute to the damage category d, RCP is the ReCiPe 2008 aggregated metric, and δ_d, ε_d are the specific normalization and weighting factors, respectively. The normalization factors are estimated based on the damage calculations for relevant European land uses, emissions and extractions [80], whereas the weighting factors are specified based on the recommended values defined in the ReCiPe 2008.

3.2.3.4. Interpretation. This phase provides an analysis of the results in addition to a set of recommendations that assist in improving the system performance. In this context, the environmental impact indicator RCP for different design alternatives is coupled with the LCC methodology which uses NPC for evaluating the future cost through a multi-objective optimization algorithm. This framework assists in optimizing the economic and environmental impacts simultaneously. As a result, a set of Pareto optimal solutions is obtained which give further insight into different design alternatives, and subsequently promote various solutions for the decision-makers that best fit their legislation.

3.2.4. Future market development criteria

In order to try to anticipate the future development of the CSHPSS technology in monetary terms taking into consideration the actual effect of the technology deployment, we performed a CSHPSS market projection up to 2030 [81–83]. The obtained learning curve by definition [84,85] tends to develop a relationship between the cumulative market size and the production cost of the CSHPSS plant (Eq. (21)).

$$C(x_t) = C(x_o) - \left(\frac{x_t}{x_o}\right)^{-b} \tag{21}$$

Here $C(x_t)$ is the marginal cost of the CSHPSS plant production (x) at a specific time t, $C(x_o)$ is the cost production at the reference point (x_o), and b is the learning parameter which is estimated based on the fractional reduction in the CSHPSS plant cost represented by the learning rate (LR). The values for the LR are estimated based on the stated recommendation in the European Energy Scenario [83]. In addition to the market projection for the next decade, several specific annual figures can be assigned so the CSHPSS cost reduction can be anticipated on a chronological index.

3.3. Optimization procedure

The main goal of the optimization procedure is to simultaneously reduce the total cost of the plant (NPC) and its environmental impact (RCP) while still satisfying the technical requirements. The decision variables in our model are the area of solar collectors (A_{COL}), and the volume of the seasonal storage tank (V_{SST}), the dimensions of the other equipment units are related to the decision variables through mathematical equations. It is worth noting that our methodology is general enough to incorporate additional decision variables.

The developed TRNSYS model is connected to the GenOpt optimization toolbox, which integrates several predefined optimization algorithms. The general mathematical representation of the simulation-optimization model can be seen below:

$$\begin{aligned} &\min_x \{f_1(x), f_2(x)\} \\ &\text{s.t. } h(x) = 0 \\ &x^L \leqslant x \leqslant x^U \\ &x \in \mathbb{R} \end{aligned} \tag{M1}$$

where $f_1(x)$ and $f_2(x)$ are the objective functions, in this case net present cost, $NPC(x)$, and ReCiPe 2008 aggregated impact factor, $RCP(x)$; x denotes the continuous variables of the simulation model, which can vary between their lower and upper bounds x^L and x^U, respectively. The equality constraints $h(x) = 0$, which correspond to mass and energy balances as well as thermodynamic correlations, are implicitly solved in TRNSYS.

The correct technical performance of the model during the optimization process is achieved by implementing a constraint to model M1. This constraint must maintain the global annual solar fraction of the system (SF) above 50% for all the optimized solutions. The modified simulation-optimization model which includes the big-M reformulation [86] is shown next:

$$\begin{aligned} &\min_x \{f_1(x) + y_1 \cdot M_1, f_2(x) + y_2 \cdot M_2\} \\ &\text{s.t. } h(x) = 0 \\ &x^L \leqslant x \leqslant x^U \\ &x \in \mathbb{R} \\ &y_1, y_2 \in \{0, 1\} \end{aligned} \tag{M2}$$

where y_1 and y_2 are the binary variables which are activated when the SF is lower than 50%, M_1 and M_2 are the big-M values corresponding to each objective function. The tightest values for the big-M are approximated using Eq. (22), where M_c stands for big-M values implemented in model M2.

$$M_c = \max\{f_c(x) | x^L \leqslant x \leqslant x^U\} \qquad \forall\, c = 1, 2 \tag{22}$$

The solution of the multi-objective problem introduced in model M2 provides a set of Pareto points, which represent the optimal trade-off between economic and environmental objectives. The extreme points of

this Pareto frontier are the so-called anchor points, which correspond to the individual minimum of each objective. The Pareto solutions are calculated here via the weighted-sum method [87], which relies on formulating an auxiliary single-objective model that optimizes a linear weighted-sum (WS) of the original objectives (M3). Note that the weighted-sum method cannot generate solutions lying on the non-convex part of the Pareto set.

$$\begin{aligned} \min_x WS &= (1-\lambda)\bar{f}_1(x) + \lambda\bar{f}_2(x) \\ &\text{s.t. } h(x) = 0 \\ &x^L \leqslant x \leqslant x^U \\ &0 \leqslant \lambda \leqslant 1 \\ &x \in \mathbb{R},\ \lambda \in \mathbb{R} \end{aligned} \tag{M3}$$

Here, $\bar{f}_1(x)$ and $\bar{f}_2(x)$ are the normalized objectives with the implemented big-M reformulation, and λ is the non-negative weight given to $\bar{f}_2(x)$, *i.e.*, the normalized $RCP(x)$ function. We normalize the objectives as shown below:

$$\bar{f}_c(x) = \frac{f_c(x) - f_c^{UT}}{f_c^{PN} - f_c^{UT}} \qquad \forall\ c = 1, 2 \tag{23}$$

where f_c^{UT} denotes the c^{th} coordinate of the utopia points and f_c^{PN} denotes the c^{th} coordinate of the pseudo nadir point. These points, f_c^{UT} and f_c^{PN}, are the anchor points.

The solution procedure was integrated via MATLAB routine designed to speed up the optimization process. The routine would launch several GenOpt toolboxes or start TRNSYS simulations whenever required.

The procedure starts with the determination of the anchor points. To obtain the individual minimum of the $RCP(x)$ function, M3 is solved for $\lambda = 1$. Next, to determine the individual minimum of the $NPC(x)$ function, M3 is solved for $\lambda = 0$. The two previous cases run simultaneously sharing all the available RAM of the computer. Once the anchor points are identified, the WS normalization is performed. Afterward, M3 is solved a finite number of times for different weight values between 0 and 1 (see details in Fig. 4) to generate the desired number of Pareto points. The MATLAB routine launches simultaneously various optimizations with different λ weights until there is no available memory. Once all the memory slots are occupied, the routine is halted until necessary RAM is liberated and then the next points are launched. The procedure ends with the display of the full Pareto frontier after all the optimization runs have met the termination criteria.

3.3.1. Optimization algorithm

To perform the separate single-objective optimization steps we used a hybrid metaheuristic optimization algorithm [55], known as the Generalized Pattern Search algorithm with Particle Swarm Optimization with Construction Coefficient and Hooke-Jeeves (GPSPSOCCHJ). This algorithm uses the combined benefits of the Particle Swarm Optimization (PSO) algorithm [88,89] and the Hooke-Jeeves (HJ) algorithm [90]. The details of this hybrid metaheuristic algorithm are discussed in Wetter [55].

The PSO algorithm is in charge of performing a global search over the feasible space of possible solutions. Since PSO is a population-based probabilistic algorithm, it generates several particles uniformly scattered over the feasible space, where each of the particles is a potential optimal solution. These potential solutions are obtained by performing runs with randomly generated values for the decision variables. On the other hand, the HJ is a local generalized pattern search algorithm, and it explores the feasible space following paths of potential minimization of the objective function. The best particle found by PSO, the potential optimal solution, is used as a starting point for the HJ algorithm, which exhaustively explores its neighborhood in an attempt to improve the solution. In order to reduce the probability of falling in a local optimum, we included multiple starts of the HJ algorithm.

This combined PSO-HJ architecture is used to avoid possible local optimal solutions which may exist due to the nonconvex nature of the problem. Note that our methodology is not limited to be used only with GPSPSOCCHJ algorithm; any other algorithm can be easily implemented.

4. Case studies (four EU climate zones)

In this section, the proposed methodology procedure was applied to four climatic zones in Europe. The objective is to assess the feasibility of the CSHPSS plant in the residential sector of these countries in techno-economic and environmental terms.

The CSHPSS plant is connected to a reference residential neighborhood community of 1120 apartments [44] which is placed in various European countries. Each apartment of this neighborhood

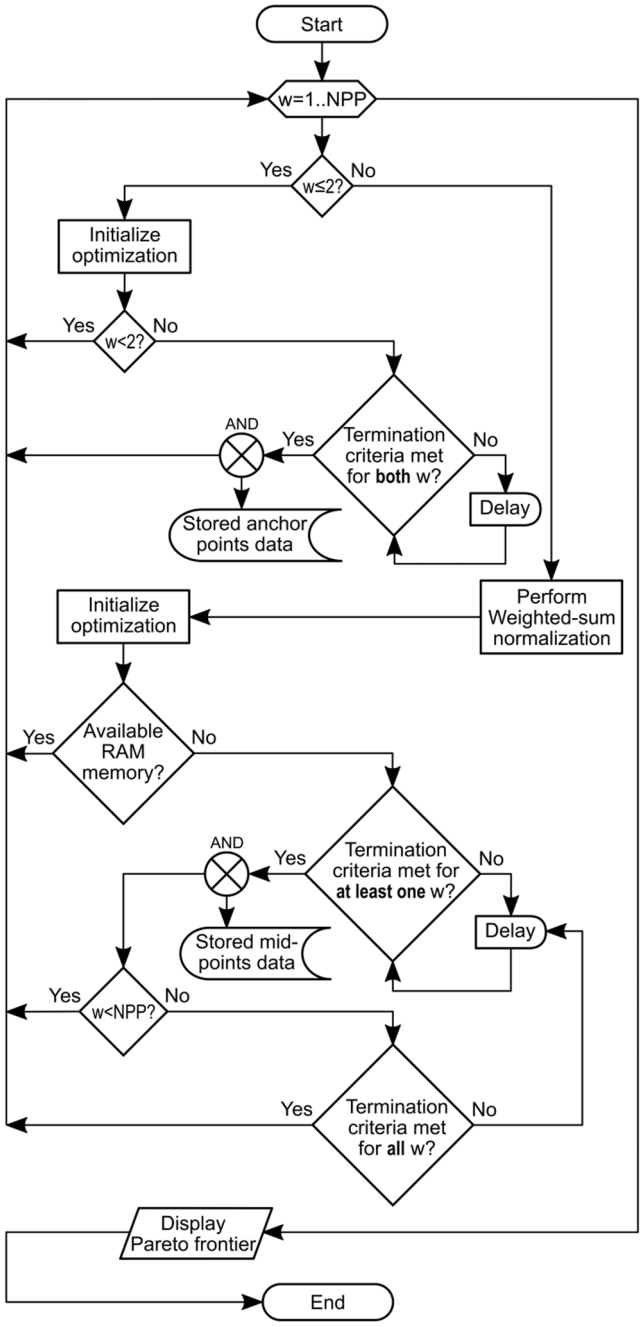

Fig. 4. Flowchart of the solution procedure performed in MATLAB environment, where NPP is the number of points of the Pareto frontier specified by the user.

community has a useful area of 90 m^2 [91]. The buildings are equipped with a radiant underfloor heating system and a domestic hot water system in order to meet the SH and DHW demand at 50 °C and 60 °C, respectively. The CSHPSS model validation is performed based on the implemented work by Guadalfajara et al. [61] and Tulus et al. [44].

Besides, a boiler fueled with natural gas is considered as a base case for comparison purposes. This conventional system is designed to satisfy the heating and DHW demand alone independently on the CSHPSS plant.

4.1. Specifications of the simulation model

A field of flat plate solar collectors supplies thermal heat to the CSHPSS model. These collectors are coupled in series and oriented to the south with a specific inclination based on the respective latitude of the cities [92] as shown in Table 1. The primary working fluid in the solar field circuit is a $67/33_{w/w}$ mixture of a water-glycol solution with a flow rate of 20 kg/h·m^2. Whereas the other three circuits (seasonal storage, SH distribution, DHW distribution circuits) are operated with water.

A partially buried tank with a cylindrical cross-section is used for a seasonal storage purpose. This tank has a fixed height to diameter ratio of 0.6, insulated with 0.5 m of extruded polystyrene and divided into 20 equally stratified levels. On the other hand, the DHW tank is relatively small since it covers only the daily DHW service. The DHWT has a height to diameter ratio of 1.7 with ten equally stratified levels.

Natural gas boilers with 93% efficiency are utilized as auxiliary heaters in both the SH and DHW distribution circuits. The boilers are designed to satisfy up to 100% of the heat demand when required.

The TRNSYS simulation predicts the transient response of the CSHPSS plant based on a simulation time step of 15 min. The system evaluation was performed over three years of simulation (28,260 h). Then the performance of the third year was extrapolated over the total lifetime of the CSHPSS plant. Due to initial homogeneity assumption of 30 °C inside the storage tanks, the first two years of simulation were performed to eliminate the initial assumption effect. The lifetime of the CSHPSS is 40 years [93]. However, the solar collectors, the DHWT, the heat exchanger, and the auxiliary heaters need to be replaced after 20 years of operation, while the lifespan of the SST is considered to reach 80 years [94].

4.2. Meteorological data

Various climate zones were selected in order to evaluate the application performance of the CSHPSS plants in the EU. In Europe, the climate can be categorized into three major climate types [95,96]: Mediterranean climate, central European climate, and Nordic climate. Four cities were selected to represent these major climatic types:

- Mediterranean climate: Madrid and Athens represent this climatic type with the difference in the daylight hours, the daily ambient temperature and the humidity due to their geographical location. Madrid is considered a Continental Mediterranean climate, while Athens is considered a Mediterranean climate.
- Central European climate: Berlin is selected as representative for this climate type. In comparison with the Mediterranean climate, a moderate reduction in the ambient temperature and daylight hours is noticed.
- Nordic climate: Helsinki is chosen as an example of this climate type. This type of weather is elected as an opposite to the Mediterranean climate with a drastic reduction in both the ambient temperature and the daylight hours.

Table 1
Latitudes and relative inclination angles of the solar collectors in the four European cities taken as representatives for the different EU climate zones.

City	Latitude (°)	Inclination angle (°)
Madrid	40	50
Athens	37	50
Berlin	52	60
Helsinki	60	70

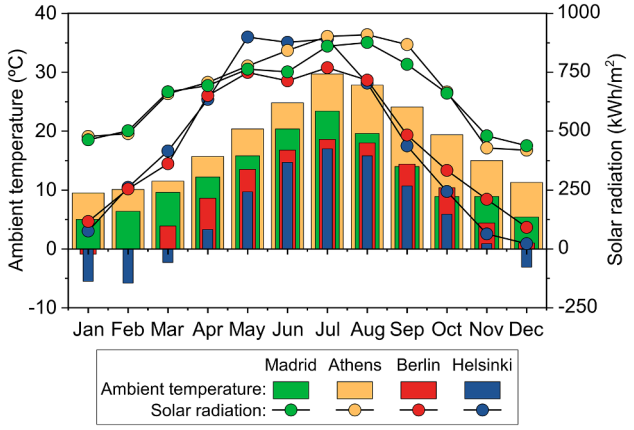

Fig. 5. Climatic conditions in the four European cities taken as representatives for the different EU climate zones.

The geographic information including the latitude and the solar collector inclination angle for the four cities are illustrated in Table 1, whereas the climate conditions of the four cities including the average ambient temperature and the annual incident solar radiation per area are extracted from the EnergyPlus database [97] as shown in Fig. 5.

Several parameters need to be defined based on the climate conditions of the cities. These parameters include the SH and DHW consumption, the economic [98] and the environmental [99] data which are defined in the following sections.

4.3. Space heating and DHW profiles

The heating demand for the residential neighborhood community follows Guadalfajara et al. [61] and Tulus et al. [44] studies. A 3-D building model was generated using a graphical tool SketchUp [100] and imported into the TRNSYS model. In TRNSYS, the occupation profiles of the apartments and physical properties of the construction materials were included. A typical hourly heating load over a year of operation depending on the climatic conditions of the city was simulated in this TRNSYS building model. These data were then extrapolated to the whole neighborhood of 40 buildings (see the profiles in Fig. 6).

The DHW demand for the residential neighborhood community depends on four main factors which comprise:

- The daily water consumption per person: Ahmed et al. [101] indicated that water consumption is highly dependent on the geographical location. Therefore, DHW consumption has a high level of diversity from one city to another. The DHW consumption per capita is 28, 30, 35, and 35 L/capita·day in Madrid, Athens, Berlin, and Helsinki, respectively [102].
- Monthly water temperature from the public distribution network: The water temperature was calculated depending on the city and the month of the year using EnergyPlus database [97].
- The number of people living in each household: The DHW consumption is dependent on the people/property value, and it is considered as a constant value (4 people/property) referring to the European average [103,104].

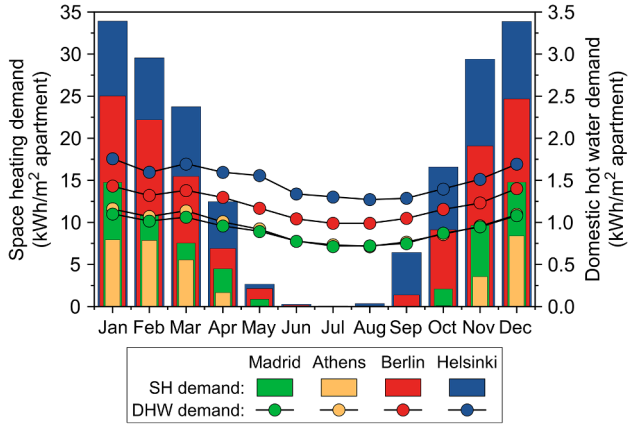

Fig. 6. Annual space heating and DHW demand profiles in the four European cities taken as representatives for the different EU climate zones.

The daily DHW consumption profiles are simulated using computer software, DHWcalc [105]. This software assists in developing a realistic and detailed hourly DHW consumption profiles with consideration for the main factors controlling the DHW demand (see the profiles in Fig. 6).

4.4. Economic and environmental data

The parameters for the initial purchase cost estimation of the main equipment units of the CSHPSS are summarized in Table 2 following Tulus et al. [44], while the operational cost is estimated at 1.5% of the initial purchase cost based on Kalogirou [66] recommendation. The cost for both the electricity and natural gas are dependent on the country policies. Therefore, the electricity and natural gas costs were extracted from the EUROSTAT database [98] and summarized in Table 4. Furthermore, the inflation rate associated with the price of these power resources is set to 5%, and 5.9% for the electricity and natural gas, respectively [44]. Additionally, the inflation rate associated with the proposed system during its life cycle is set to 2.3% [106], while the annual discount rate is set to 3.5% [107].

The LCA data are retrieved from the Ecoinvent database [99]. These data include the impact of various CSHPSS equipment units (Table 3) and utilities (Table 4) based on the ReCiPe 2008 methodology.

The pollution associated with the extraction of natural gas from the underground reserves should be limited in the proposed system. On the other hand, the pollution associated with the electricity generation is highly dependent on the electricity mix of the specific country. Therefore, the natural gas environmental impact is considered the same for the selected cities, while the electricity impacts are variable, as indicated in Table 4.

4.5. Future market development data

By the end of 2016, the cumulative capacity of the installed solar heating systems in Europe increased by 2.6% compared to the previous year to achieve a total installed capacity of 34.5 GW_{th}. Germany has the lead in the solar heating systems installation in Europe where a 0.52 GW_{th} within 2016 was added to a total capacity of 13.14 GW_{th}. Elsewhere in Europe, Spain added a 0.146 GW_{th} to achieve a total capacity of 2.4 GW_{th}, whereas Greece and Finland added 0.19 GW_{th} and 0.0028 GW_{th} [14].

The future market of the CSHPSS based on an in-depth analysis of solar heating energy systems from the technical, social and political perspectives, shows different expansion scenarios for this technology in Europe. Greenpeace international [108] proposed the EU 27 energy scenario for the CSHPSS expansion up to the year 2030 as shown in Table 5.

Besides, the natural gas price trends are assumed to increase in a moderated manner based on the recommendations of the Federal Ministry of Environment of Germany [109] (see Table 5). These trends are motivated by the shortage in the CO_2 allowance [110].

The forecast cost for the CSHPSS technology can be generated based on the observed historical learning rate of solar thermal collector systems over the forecasted period between 2020 and 2030. The learning rate of such systems is 0.90 according to Greenpeace international [83].

Table 3
Aggregated ReCiPe 2008 impact factor for the CSHPSS equipment units, in ReCiPe points (Pt) per characteristic dimension.

Unit	ReCiPe 2008 impact factor (final score)
Solar collector	17.0 Pt/m^2
Storage tank	117 Pt/m^3
Auxiliary boiler	$1.57 \cdot 10^3$ Pt/unit
Heat exchanger	9.00 Pt/m^2
Pump	82.0 Pt/unit

Table 4
Specific costs and aggregated ReCiPe 2008 impact factors for the utilities in the four European cities taken as representatives for the different EU climate zones.

City	Electricity		Natural gas	
	Cost (€/kWh)	Impact (Pt/kWh)	Cost (€/kWh)	Impact (Pt/kWh)
Madrid	0.101	0.0357	0.0294	0.0230
Athens	0.0862	0.0193	0.0242	0.0230
Berlin	0.0761	0.0529	0.0277	0.0230
Helsinki	0.0596	0.0261	0.0296	0.0230

Table 5
Estimated growth of CSHPSS installed capacity according to Greenpeace International and projected increase of the natural gas price up to 2030.

Parameter	2017	2020	2025	2030
Total installed capacity (GW_{th})	34.50	40.66	52.77	67.16
Average EU natural gas price (€/kWh)	0.02700	0.03200	0.03415	0.03630

5. Results and discussions

In this study, the results are presented in four main parts. The first part depicts the behavior of CSHPSS in one of the proposed EU climate zones. Then, in the second part, the discussion is extended to the other three cities. These two parts provide a detailed analysis of techno-economic and environmental characteristics based on a set of Pareto

Table 2
Purchase cost parameters of the CSHPSS equipment units [44].

Unit	α_k	β_k	CAP_k	Range	Base year	FBM_k
Solar collector	974.2	0.8330	Aperture area (m^2)	4000–15,000 m^2	2007	1.00
Storage tank	3955	0.6500	Volume (m^3)	1–100,000 m^3	2007	1.00
Auxiliary heater	225.0	0.7460	Duty (kW)	600–10,000 kW	2001	2.10
Heat exchanger	3.133	−0.3310	Exchange area (m^2)	10–1000 m^2	2001	3.29
Pump (P_1, P_2)	389.0	−283.2	Mass flow rate (kg/h)	15,000–100,000 kg/h	2009	3.24
Pump (P_3, P_4)	389.0	717.0	Mass flow rate (kg/h)	15,000–100,000 kg/h	2009	3.24

optimal solutions in comparison to a conventional heating system fueled by natural gas (base case). Next, the main results are expressed along with an appropriate sensitivity analysis for the proposed optimal solutions of the system. Finally, the market projection forecast for the CSHPSS is portrayed using historical learning rates.

5.1. Application analysis (Madrid case study)

The capabilities of the formulated multi-objective optimization model are illustrated through Madrid case study that addresses the design of CSHPSS in the Mediterranean EU climate zone. A set of optimal solutions that define the Pareto frontier are obtained as a result of the optimization process (see Fig. 7). Each point of the Pareto front comprises a defined configuration of the CSHPSS plant under a set of operational conditions. The average computation time for the anchor points was 15,700 CPU seconds (8 execution units of 2.0 GB RAM each for every anchor point, optimizing both simultaneously) and 47,000 CPU seconds for the intermediate Pareto solutions (2 execution units of 2.0 GB RAM each for every intermediate point, optimizing all of them simultaneously) using an Intel® Xeon® E5-2620 v4 2.10 GHz processor with 32.0 GB RAM.

As observed in Fig. 7, there is a clear trade-off between the proposed objective functions since the reduction in the environmental impact can be only achieved through an increment in the expenses of the CSHPSS plant. The projected optimal solutions, following our methodological framework, visibly improve the environmental impact in comparison to the base case. Point A and B are the optimal design Pareto points with minimum cost and impact, respectively. Note that these points consider the integration of solar thermal energy storage. Replacing the base case with a CSHPSS plant following point A configuration can reduce the environmental impact by 81.1%, whereas point B reduces it even more, by 86.5%. On the other hand, the Pareto optimal systems could not provide a marginal economic reduction compared to the base case. The installation of a CSHPSS in these cases corresponds to an increase in the cost of approximately 1% and 6.1% in A and B cases, respectively compared to the base case.

In the optimal minimum cost solution (point A), the *NPC* is equal to 52.6 €/MWh which is smaller than solution B by 4.7%, whereas in the minimum impact solution (point B), the *RCP* is 3.34 Pt/MWh which is smaller than solution A by 28.6%. Besides, point C embodies one possible intermediate Pareto optimal solution where the *NPC* is equal to 53.3 €/MWh, and the *RCP* reaches 3.6 Pt/MWh, this intermediate point increases the economic cost by 1.25% compared to the point A, but simultaneously reduces the environmental impact by 23.1%. It is worth noting that point C is selected as an example solution for comparison purposes. Likewise, any other intermediate solution could be selected since all of them are Pareto optimal.

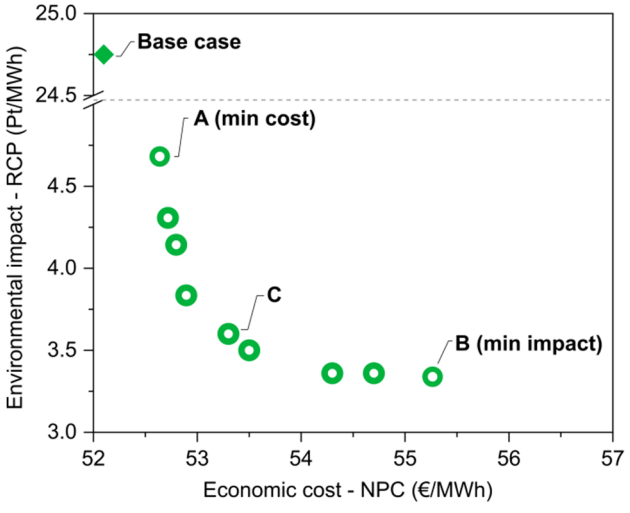

Fig. 7. Pareto set of optimal solutions for the CSHPSS in Madrid which covers 7654 MWh/year of combined SH and DHW demand during its lifetime. Anchor point A is the minimum cost solution, anchor point B is the minimum impact solution, and the intermediate point C is one of the trade-off solutions with $\lambda = 0.44$ (weight) given to the normalized environmental impact objective function, the $RCP(x)$; the base case represents a natural gas heating system.

Following that, each point in the Pareto set represents a different configuration of the CSHPSS plant. The proposed methodology offers the possibility to perform a detailed analysis of any Pareto optimal solution. Here we analyzed the anchor points (point A and B) from the economic and environmental perspectives comparing them to the base case.

5.1.1. Economic cost analysis

To facilitate detailed economic analysis, Fig. 8 provides a comprehensive breakdown of the cost contribution of each parameter for the

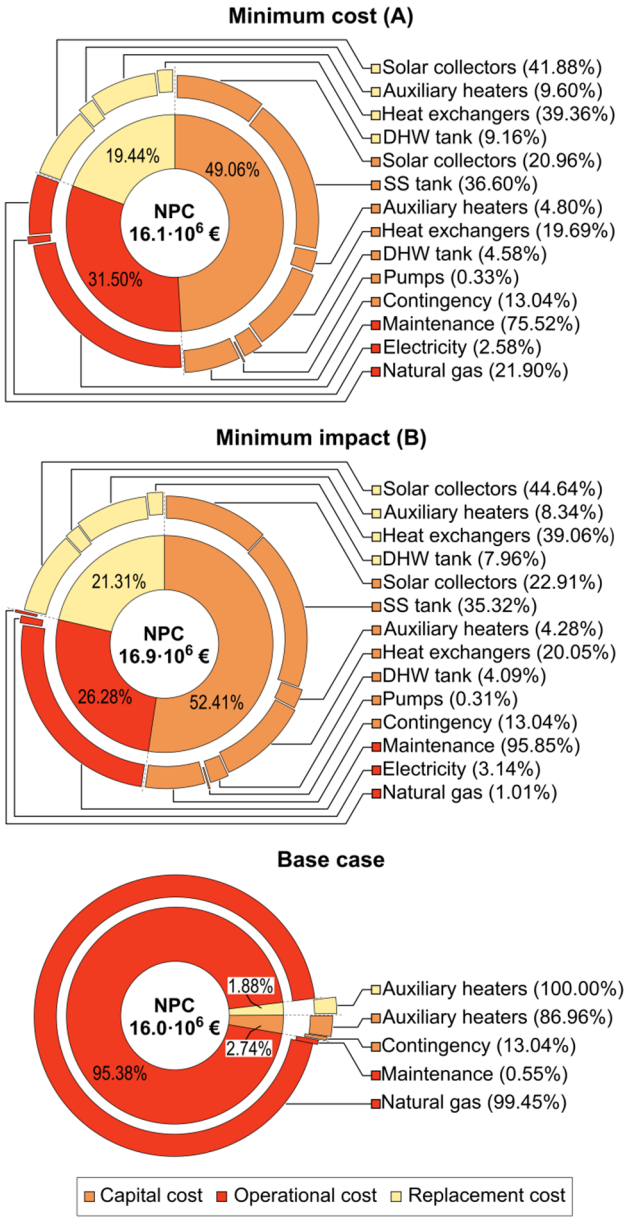

Fig. 8. Distribution of the net present costs of two Pareto optimal solutions (point A and B in Fig. 7) for the CSHPSS in Madrid which covers 7654 MWh/year of combined SH and DHW demand during its lifetime and the base case, which represents a natural gas heating system.

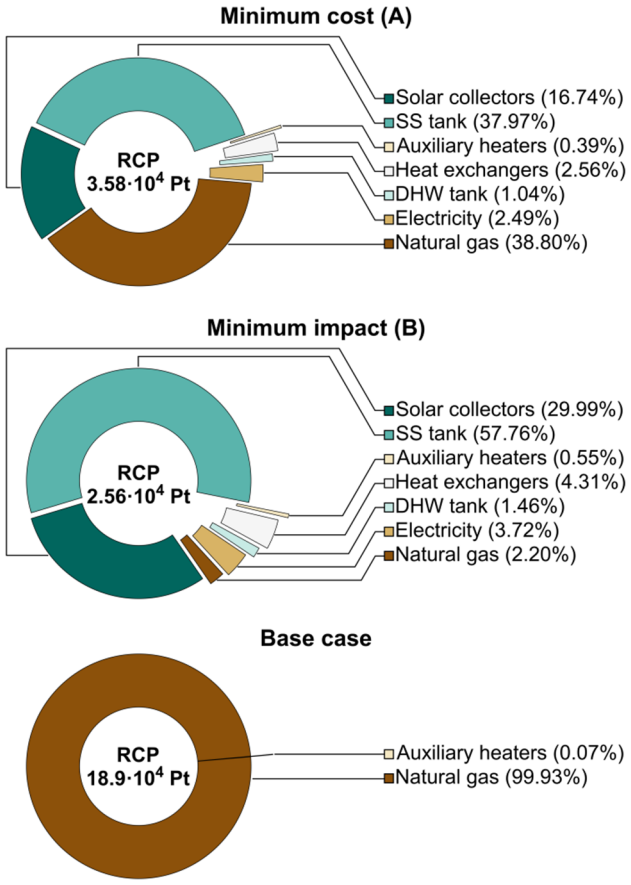

Fig. 9. Distribution of the aggregated ReCiPe 2008 environmental impact of two Pareto optimal solutions (point A and B in Fig. 7) for the CSHPSS in Madrid which covers 7654 MWh/year of combined SH and DHW demand during its lifetime and the base case, which represents a natural gas heating system.

Pareto optimal solutions A and B during their operation life together with the base case solution. In this figure, the initial capital cost, associated with both A and B solutions, has a significant contribution compared to the base case. This contribution is 49.06% and 52.4% in solution A and B, respectively, whereas in the base case, it is only 2.73%. This marginal capital cost contribution is commonly arisen in the CSHPSS plants due to the deployment of the solar energy in a district heating field which requires a high investment cost [22]. To be more specific, the solar collectors and SST represent 28.24% and 30.52% of the capital cost for the Pareto optimal solution A and B, respectively. The minimum cost solution (A) has solar collector field of 6888 m^2 and SST of 65784 m^3, whereas the minimum impact solution (B) has solar collector field 8802 m^2 and SST of 74322 m^3. Since the DHWT is used only for the daily services without seasonal storage, it represents almost about 4.5% of the initial capital cost in both the Pareto optimal solution A and B with a tank size of 109.6 m^3. The same behavior was noticed for replacement cost which represents 19.4% and 21.3% in solution A and B compared to only 1.88% in the base case. On the contrary, the operational cost has a predominant contribution of 95.4% in the base case compared to 31.5% and 26.3% in the optimal solutions A and B, respectively. Such a high operational cost is due to the dependency of the base case on natural gas cost. In general, solution A and B have a similar distribution for the *NPC* components. However, the minimum cost solution (A) has a slightly higher contribution of 6.9% for the natural gas compared to the minimum impact solution with only 0.27% which will be reflected in the environmental impact analysis.

5.1.2. Environmental impact analysis

As shown in Fig. 9, solution A and B success in declining the environmental impact up to 7 times compared to the base case due to the deployment of the solar water heating systems and the saving of non-renewable energy systems (*i.e.*, natural gas and electricity). In the base case, the natural gas represents almost 100% of the environmental damage ($1.88 \cdot 10^5$ Pt). While this contribution is reduced to 38.8% ($1.39 \cdot 10^4$ Pt) in the minimum cost solution (A) and it becomes almost negligible in the minimum impact solution (B) where it counts only for 2.20% ($5.60 \cdot 10^2$ Pt).

Following the economic analysis of the anchor points (A and B), the solar collector and the SST share most of the contribution to the total environmental impact [63]. In solution A, the solar collector counts for 16.7% of the total damage to the environment, whereas this fraction increases up to 30% in the solution B due to the limitation of using natural gas as the primary fuel. On the other hand, the impact fraction of the SST represents 37.9% in solution A, and it increases to 57.7% in solution B.

As the latest highlight, the impact of the heat exchangers increased by 40.1% from solution A to B. This is due to the further deployment of the solar collectors in the minimum impact solution (B), and subsequently extra supplement of heat exchange is required to cover the additional solar energy.

5.1.3. Energy analysis of an intermediate Pareto optimal solution (C)

The thermal performance characteristics of the optimized CSHPSS plant configuration based on the proposed methodological framework is presented through an intermediate Pareto optimal solution (point C in Fig. 7). This solution is designed to fulfill a total SH and DHW demand of approximately 6555 MWh/year and 1099 MWh/year, respectively. Note that any other intermediate point in the proposed Pareto set would be similarly comparable in this analysis.

As shown in Fig. 10, the monthly amount of SH and DHW demands are mainly covered by the solar collectors and the thermal energy stored in the SST and the DHWT. In Fig. 10 the energy supplied by the CSHPSS plant is represented as a positive input, whereas the energy stored in the SST is depicted as a negative input.

In summer and autumn seasons (*i.e.*, April to October), when the solar radiation is relatively high, and the SH demand is small, most of the provided energy from the solar collectors are directly stored into the SST, and the remaining is utilized to cover the instant heating demand. On the contrary, the solar radiation decreases, and the heating load significantly increases during the winter season (*i.e.*, November to January), therefore the total demand is covered through a combination of the energy supplied by the DHWT, the solar collectors and the stored energy in the SST. Moreover, in extreme cases when the proposed solar system fails in fulfilling the required heating demand, the auxiliary heaters fueled by natural gas deliver the necessary energy. These cases happen during February and March where most of the stored energy in the SST is already discharged during the coldest months. This can be reflected in the solar fraction of the distribution circuits during these months. In February, the solar fraction declines by 5.84% and 1.22% for the SH and DHW circuits, respectively. While in March, this value changes a bit for the DHW distribution circuit and the solar fraction increases by only 2.81% due to the increment in the solar radiation. On the other hand, the solar fraction for the SH circuit keep deteriorating, and it drops by 10.1% due to the absence of the seasonal storage and the limited direct energy provided by the solar collectors.

5.2. Application analysis on the selected climate zones in the EU

Following Madrid case analysis combined with the main objective of assessing the CSHPSS plant feasibility in the residential sector at various climate zones in the EU, the proposed methodological framework correspondingly based on the multi-objective approach is applied to optimize the cost against an aggregated environmental metric in

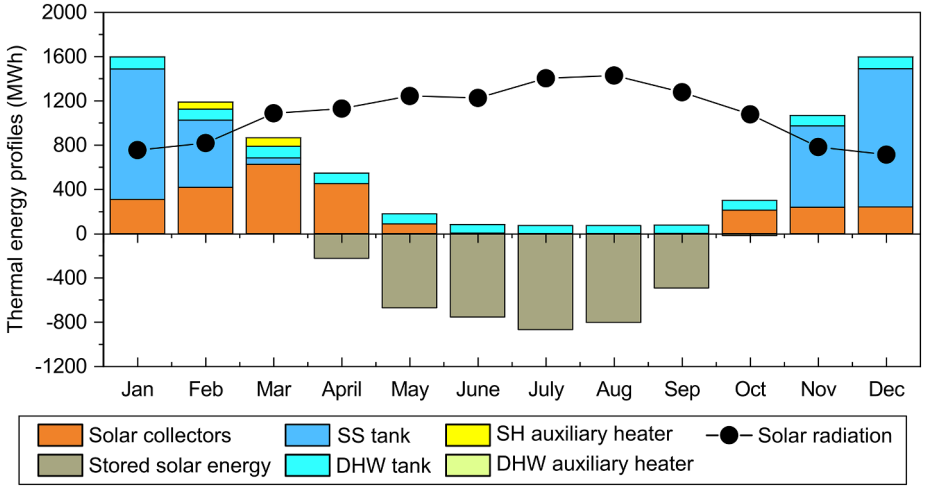

Fig. 10. Annual thermal energy profiles of an intermediate Pareto optimal solution (point C in Fig. 7) for the CSHPSS in Madrid which covers 7654 MWh/year of combined SH and DHW demand during its lifetime.

Athens, Berlin and Helsinki as a representative for the Mediterranean, central European, and Nordic climates, respectively. The problem is formulated to cover annual SH and DHW demands of 4661 MWh, 14,180 MWh, and 20,896 MWh for Athens, Berlin, and Helsinki, respectively.

As shown in Fig. 11, a clear trend is observed for the deployment of the CSHPSS which causes a rise in the economic cost under various EU climate zones compared to the base cases. The optimal economic solutions in the nominated locations depend on several factors including the climate condition, the heating demand, and the natural gas and electricity prices. In Athens, the *NPC* in the minimum cost and impact optimal points have been raised by 33.3% and 50.8%, respectively compared to their base case. This high growth is due to the low cost of non-renewable energy resources in Athens compared to Madrid. Following the observed tendency in Athens, the *NPC* in Berlin case raised by 16.9% and 25.3% compared to their base case. On the other hand, the *NPC* increase only by 3.12% and 8.11% in Helsinki due to several factors including, the high price of natural gas and electricity, and the high heating demand.

The optimal environmental solutions for the four locations follows the minimum impact solution of Madrid case where the *RCP* improves by 84.7%, 82.1%, and 82.9% for Athens, Berlin, and Helsinki cases, respectively. The same tendency was found for Berlin and Helsinki at the minimum cost solution since the *RCP* improved by 71.3% and 77.9% for Berlin and Helsinki. On contrary, the low natural gas and electricity prices in Athens restrict substantial improvement in the *RCP*, and it is improved only by 42.9%. This marginal improvement in the minimum cost optimal solution of Athens case will be mirrored in its breakdown for the *NPC* and *RCP*.

5.2.1. Economic cost analysis for the EU climate zones

Fig. 12 shows a comprehensive breakdown of the *NPC* of various CSHPSS plants during their lifetime under different EU climate zones. Similar contributions can be observed for each component of the *NPC* comparing among Madrid, Berlin and Helsinki cases. Furthermore, the results show that the capital and replacement costs for the presented optimal solutions (minimum cost and minimum impact) of Berlin and Helsinki are quite large in comparison to their base cases as mentioned in Madrid case study. Moreover, the results confirm the dependency of the CSHPSS plant configuration on the heating demand where the capital and replacement costs ascending increases with the heating demand based on the climate zone [48] as shown in Madrid, Berlin, and

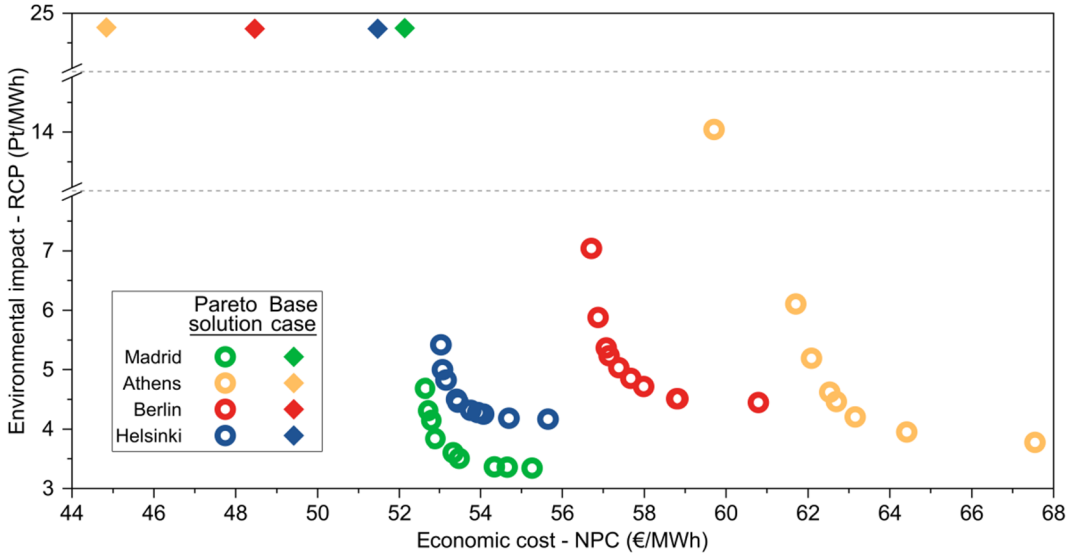

Fig. 11. Pareto sets of optimal solutions for CSHPSS plants in various EU climate zones covering specific SH and DHW yearly demands; the base cases represent natural gas heating systems.

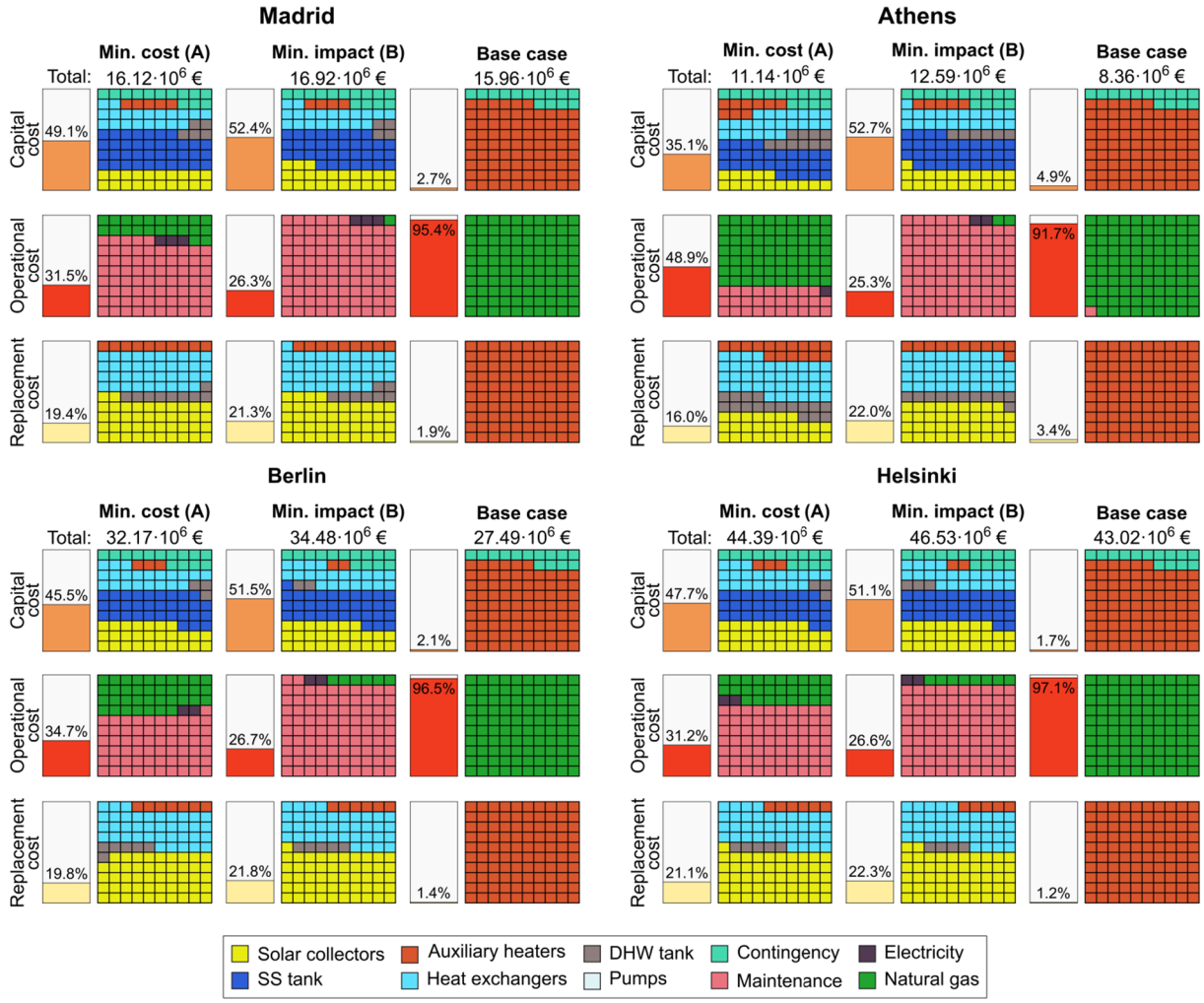

Fig. 12. Breakdown of the net present cost including the shares of initial capital cost, operational cost, and replacement cost for Pareto optimal anchor solutions (minimum cost and impact) of CSHPSS plants under different EU climate zones in comparison to their respective base cases.

Helsinki, respectively.

On the contrary, the low heating demand combined with the low prices for the natural gas and electricity in Athens contribute to change the distribution for the *NPC* of the minimum cost optimal solution in this Mediterranean zone. The operational cost has a significant contribution of 48.9% compared to only 35.1% of the initial capital cost and 16% of the replacement cost. This is due to the dependency of the system on natural gas which almost represents 69.6% of the operational cost and the limited involvement for the solar water heating system. More precisely, the solar collectors and SST represent only 15.7% and of the initial capital and 27.2% of the replacement costs. In term of the renewable energy equipment sizing at the proposed climate zones, Table 6 shows a summary for the proposed sizing the renewable energy equipment based on the Pareto optimal solution in various EU climate zones. It is noticed that for all the minimum impact optimum solutions under different EU climate zones, the ratio between the SST volume and the solar collector field area is around 8 ± 0.5 m^3/m^2 for the minimum impact solutions based on the climate zone.

5.2.2. Environmental impact analysis for the EU climate zones

Fig. 13 shows a breakdown for the environmental impact into its categories for the minimum cost and impact Pareto optimal solutions of a CSHPSS plant under different climate zones in comparison with its base case. The results follow the environmental impact breakdown of Madrid where the optimal solutions can reduce the environmental impact up to 5.5 and 5.8 times for Berlin and Helsinki cases, respectively. In Athens

Table 6
Optimal CSHPSS equipment sizing of the Pareto anchor solutions in different EU climate zones.

City	Optimal solution	Area of solar collectors (10^3 m^2)	Volume of seasonal storage tank (10^3 m^3)	Volume of domestic hot water tank (m^3)	V_{SST}/A_{COL} ratio (m^3/m^2)
Madrid	A	6.888	65.78	109.7	9.55
	B	8.802	74.32	109.7	8.44
Athens	A	2.097	15.25	117.6	7.27
	B	5.593	44.39	117.6	7.94
Berlin	A	21.00	149.2	137.2	7.10
	B	25.50	198.0	137.0	7.76
Helsinki	A	32.91	230.4	168.5	7.00
	B	38.13	287.9	168.5	7.55

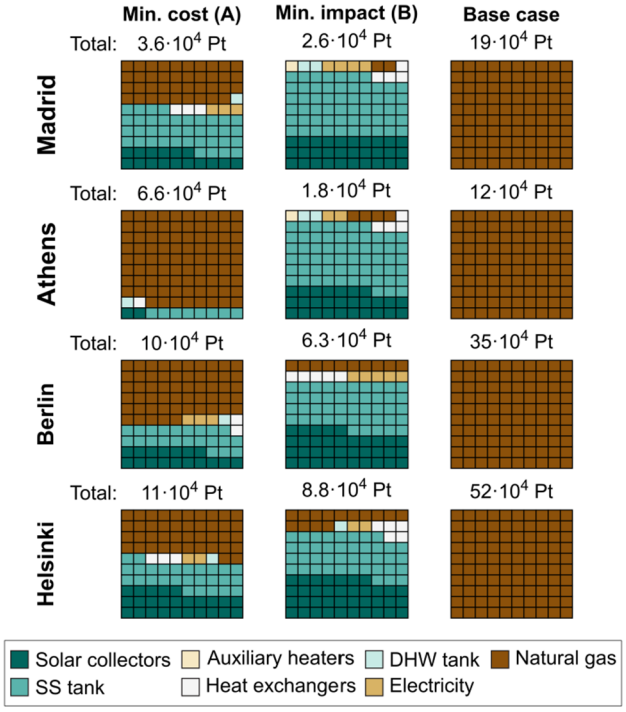

Fig. 13. Breakdown of the aggregated ReCiPe 2008 environmental impact of Pareto optimal anchor solutions (minimum cost and impact) of CSHPSS plants under different EU climate zones in comparison to their respective base cases.

case, the minimum cost optimal solution reduces the environmental impact only by 1.75 times. This relatively small reduction is due to the significant contribution of the natural gas ($5.7 \cdot 10^4$ Pt) which represents almost 87.5% of the total environmental impact.

Following the environmental impact in Madrid case, the solar collector and SST are the main contributor to the total environmental impact in the minimum cost optimal solution with a contribution of 39.6%, and 52.7% in Berlin and Helsinki, respectively. This contribution increases significantly for the minimum impact optimum solutions, where they share 87.2%, 80.2%, and 78.9% in Athens, Berlin and Helsinki solutions, respectively.

5.2.3. Energy analysis for the EU climate zones

Following the energy analysis in Madrid case study, an intermediate Pareto optimal solution with $\lambda = 0.44$ is presented to evaluate the thermal performance of the CSHPSS plant in different EU climate zones as shown in Fig. 14.

Table 7
Annual space heating (SH) and domestic hot water (DHW) solar fractions of intermediate Pareto optimal solutions with $\lambda = 0.44$ in various EU climate zones.

City	SF_{SH} (%)	SF_{DHW} (%)
Madrid	97.8	98.9
Athens	90.1	97.4
Berlin	95.2	84.9
Helsinki	97.5	74.7

Based on the limitation of the solar heating system in covering the heating demand during several months in Berlin and Helsinki, the AUX_1 operated from February until April due to the full discharging of the SST during the winter period. Furthermore, the AUX_2 almost operates throughout the year except the summer months (June to August) for these climates since the DHW tank is designed to cover only the daily services. In Athens, limited seasonal storage is projected between April and October where high solar radiation and low heating demand are observed due to the Mediterranean weather conditions (see Figs. 5 and 6). This limited heating demand reduces the usage of auxiliary heaters throughout the whole year.

Based on normalizing the technical performance of the CSHPSS plant, the solar fraction was presented, and its minimum value was noticed during January and March for the DHW and SH circuits, respectively. In the DHW distribution circuit, the solar fraction is 62.1% and 47.5% for Berlin and Helsinki, respectively. While the solar fraction for the SH distribution circuit becomes 74.1% and 84.5% in Berlin and Helsinki, respectively. On the other hand, due to the low price of natural gas in Athens in comparison to the other EU countries, an extensive usage for the auxiliary heaters in March is shown where the solar fraction has reduced to 54.6% for the SH circuit and sustain around 98.7% for DHW circuit due to low DHW heating demand. Even though the literature shows a high variation in the solar fraction when the CSHPSS plants introduced under different climate zones, the proposed methodological framework succeeds in reducing the solar fraction variation when introduced in various climate zones as shown in Table 7. In the SH distribution circuit, which has a substantial contribution to the life cycle of the CSHPSS plant, the solar fraction never goes below than 90% for different EU climate zones. While due to the DHW distribution circuit functionally in covering only the daily services, the solar fraction diminishes up to 74.7% in Helsinki due the high demand in the winter period.

Remarking that the proposed optimal solutions for the CSHPSS plants in different EU climate zones are high sensitivity for their geographical locations and economic parameters comprise energy prices. Therefore, the influence of the most relevant economic parameters

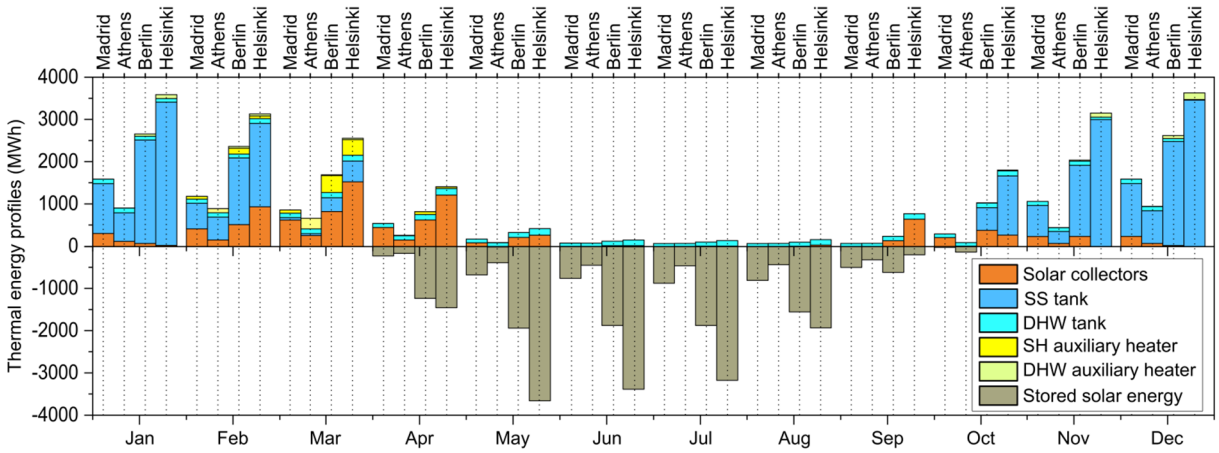

Fig. 14. Annual thermal energy profiles of intermediate Pareto optimal solutions with $\lambda = 0.44$ in various EU climate zones covering specific SH and DHW demands.

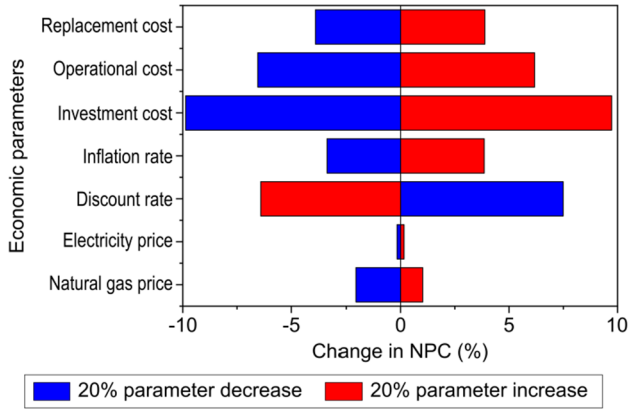

Fig. 15. Sensitivity analysis, which shows the effect of different economic parameters on the net present cost of the optimized minimum cost Pareto solution in Madrid case study (point A in Fig. 7).

should be assessed in a sensitivity analysis to give an estimate for the uncertainty associated with the results.

5.3. Sensitivity analysis for the methodological framework

A sensitivity analysis for the most critical economic parameters is implemented to understand their influence on both the *NPC* and *RCP* objective functions. This analysis is carried out based on One-factor-at-a-time (OFAT) approach [111] in which each economic parameter is varied by up to 20% after another in comparison to a reference case. The Pareto optimal solution (A) of Madrid case study is selected as the reference case. The assessment includes the influence of the natural gas price, electricity price, discount rate, inflation rate, investment cost, operational cost, and replacement cost. The sensitivity analysis not only comprises the influence of the selected parameters on the *NPC* and *RCP*, but it also proposes a detailed breakdown for the economic cost and the environmental impact for the influence of each of these parameters.

Aligning with the financial challenges facing the CSHPSS plant, Fig. 15 shows the sensitivity analysis for a CSHPSS plant configured based on the optimal solution A (minimum cost) under Madrid climate zone demonstrates a high dependency for the *NPC* on the investment cost followed by the discount rate and the operational cost in which it can changes up to 9.8%. This change can be explained through the change in the system configuration where the reduction in the discount rate and the investment cost aggravate a slight more dependency on using renewable energy sources. Furthermore, a non-linear effect for both the natural gas price and the discount rate is noticed. The *NPC* changes by 1.02% and 2.05% for increasing and decreasing the *NPC* by 20%, respectively. On the hand, the *NPC* increases by 7.49% for decreasing the discount rate by 20%, whereas it decreases only by 4.30% for increasing the discount rate by 20%. The inflation rate and the replacement cost have a limited contribution to the *NPC* since it changes only by 3.8% for both. The electricity price has a minor influence on the *NPC* since it has a marginal share of the total cost in the reference case.

Fig. 16 (to the left of the reference case) shows a breakdown for reducing the economic parameters of the optimal solution A by 20% where each component of the bar comprises the share percentage of a certain cost parameter in the *NPC* breakdown. The *NPC* breakdown shows the changes in the system configuration due to the reduction in the natural gas price. This reduction intends to propose the natural gas usage as a visible solution instead of the solar water heating system in covering the heating demand. Therefore, a large share of 38% is observed when the natural gas price decrease 20%, respectively. On the contrary, the natural gas in the reference case shares only 6.89%. Furthermore, the large share of natural gas reduces the use of solar collectors to only 11.9% and the SST to 9.87%, whereas the reference case shares up to 18.4% and 17.9% of the total shared solar collectors and SST, respectively. For the breakdown of increasing the economic parameters of the optimal solution A by 20% shown in Fig. 16 (to the right of the reference case), almost the same pattern is observed for changing the discount rate and the investment and operational costs with a slight change in the natural gas share.

Following the sensitivity analysis for the *NPC* objective function,

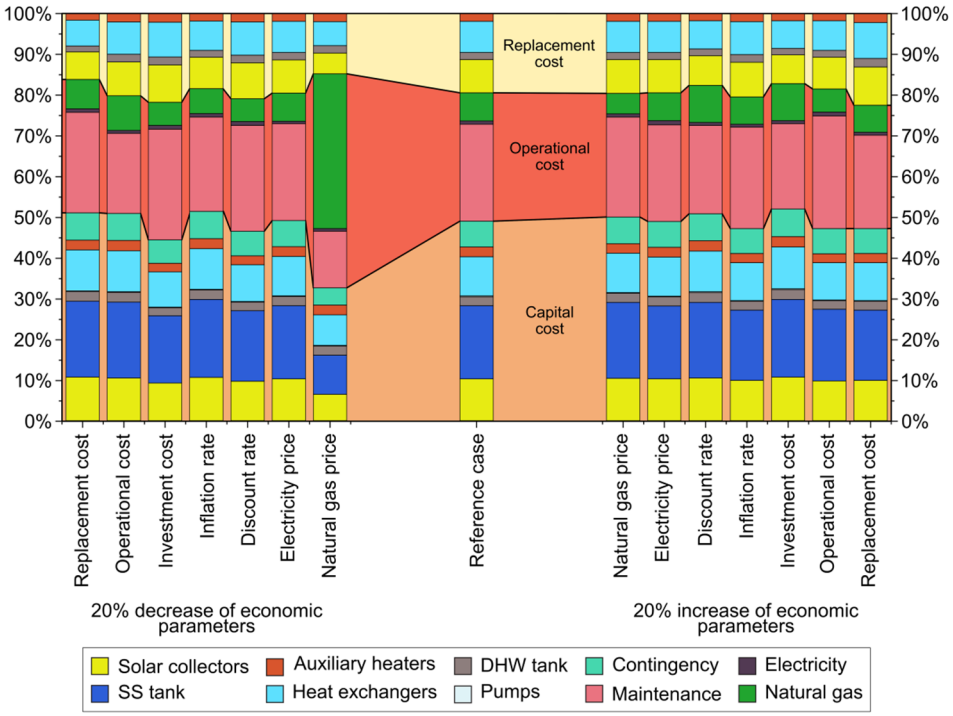

Fig. 16. Breakdown of the sensitivity analysis data for Madrid case study shown in Fig. 15, which depicts the distribution of the net present cost components when the economic parameters are decreased (to the left of the reference case) and increased (to the right of the reference case) by 20%.

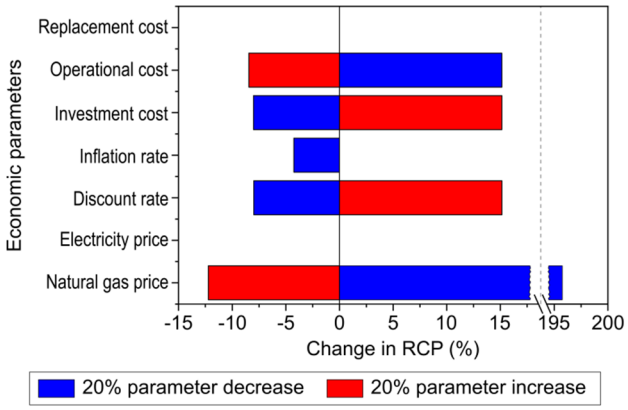

Fig. 17. Sensitivity analysis, which shows the effect of different economic parameters on the aggregated ReCiPe 2008 environmental impact of the optimized minimum cost Pareto solution in Madrid case study (point A in Fig. 7).

Fig. 17 shows the sensitivity analysis for the *RCP* when the economic parameters vary by 20%. Recalling the sharp influence for the natural gas price in presenting the natural gas usage as a valid solution with a limited share for the solar collectors and SST, the *RCP* increases 195.7% for reducing the natural gas price. Moreover, when this parameter increase 20% and due to the non-linear noticed effect, the *RCP* decreases by 12.2%. On the other hand, the discount rate and the investment and operational costs have a slight effect in the *RCP* since it increases by 15.14% when the investment cost and discount rate increased by 20%. While increasing the operational cost promote a reduction in the *RCP* by 15.14% due to the slight dependency of using renewable energy sources.

The dramatic increase in the *RCP* for the reducing the natural gas price can be observed in the *RCP* breakdown which is shown in Fig. 18 (to the left of the reference case). A high dependency is noticed when using natural gas instead of the solar water heating system where the natural gas shares 88.4% for varying the natural gas price down 20%, whereas the natural gas shares only 38.8% in the reference case. On the other hand, increasing the economic parameters 20% keeps almost the share for each parameter as the reference case with a marginal change in the natural gas share when the natural gas increases 20%, as shown in the *RCP* breakdown Fig. 18 (to the right of the reference case).

5.4. Discussion and future market development

The future potential of CSHPSS plants in different EU climate zones is assessed through various Pareto optimal solutions offered by the proposed methodological framework in which both the techno-economic and environmental impact is considered. Generally, the CSHPSS system succeeded in decreasing the environmental impact in the investigated climate zones. However, the high investment cost of the CSHPSS plants compared to the conventional heating systems that use natural gas as fuel limit the extended benefit of wide-spreading the CSHPSS plants in different EU climate zones.

This limitation becomes more substantial in Athens (Mediterranean climate zone) where heating demand is low due to the high solar radiation throughout the year, and the prices of the non-renewable energy resources are low. However, the growing tendency for the natural gas price in the EU [109] would positively affect the economic feasibility of the CSHPSS plants in different EU climate zones. Therefore, as a part of the methodological framework, the future development in the plant cost with consideration for the actual effect of the technology deployment is evaluated for the proposed EU climate zones based on the historically observed learning curves.

As shown in Fig. 19, a clear trade-off for the increment in the conventional systems price is observed, this price raise associates with a gradual declination in the CSHPSS plants prices. In the long term, the CSHPSS plants in various EU climate zones can significantly underprice the *NPC* in comparison to the conventional system using natural gas by 2030. This development can significantly assist in improving the competitiveness of the CSHPSS plant as a sustainable alternative solution in

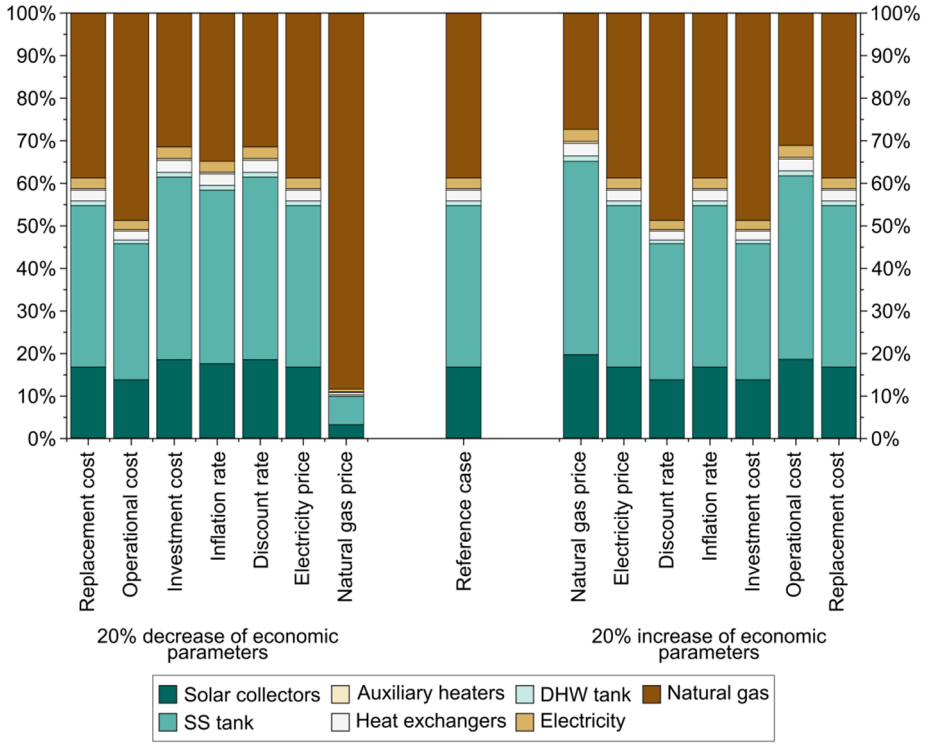

Fig. 18. Breakdown of the sensitivity analysis data for Madrid case study shown in Fig. 17, which depicts the distribution of the aggregated ReCiPe 2008 environmental impact when the economic parameters are decreased (to the left of the reference case) and increased (to the right of the reference case) by 20%.

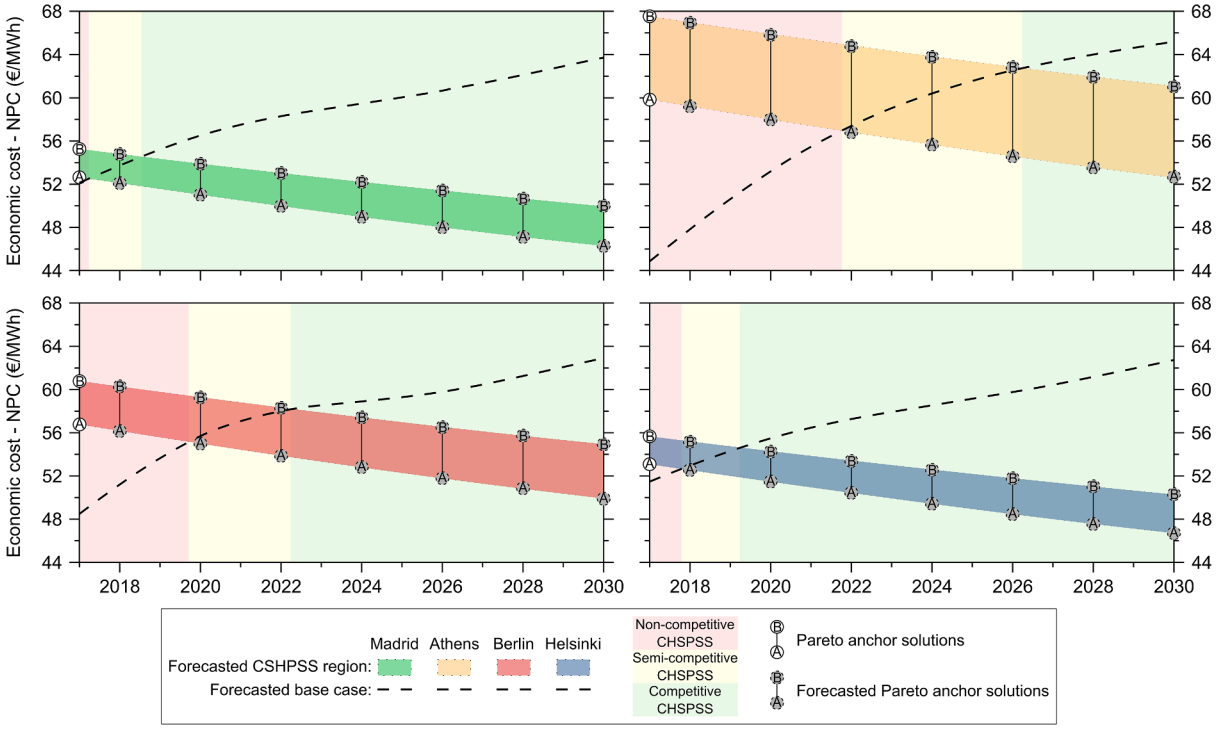

Fig. 19. Forecast projections of the net present costs of optimized CSHPSS plants in different EU climate zones along with their base cases (natural gas heating systems). The colored areas between A and B anchor points represent the distribution of the Pareto optimal solutions in time, whereas the black dashed lines are the future projections of the base cases. The vertical color zones show the expected competitiveness of CSHPSS plants compared to the base case, from red (non-competitive) to green (competitive).

comparison to the conventional systems.

Currently, in Madrid, the CSHPSS plants can cover the heating demand for less than 52.6 €/MWh, whereas its base case covers it at 52.1 €/MWh. With this minor difference, the feasibility of the CSHPSS plant under Madrid climate conditions can be proved. In 2030, the *NPC* will range from 46.3 to 49.9 €/MWh for the CSHPSS while its base case 63.7 €/MWh. In Athens where the CSHPSS plant can cover the heating demand at high price ranged between 59.7 and 67.5 €/MWh. Beyond 2022, the CSHPSS plants will be able to cover the heating demand at a lower cost than the conventional system, at which the heating demand is covered at a price of 56.7 to 64.8 €/MWh. The CSHPSS plant in Athens will continue decreasing to less than 52.5 €/MWh by 2030, whereas the base case will increase to 65.2 €/MWh. In Berlin, a slight cost reduction would be available in the CSHPSS plants by 2020 where the *NPC* will range from 54.9 to 59.3 €/MWh. By 2030, the CSHPSS plant *NPC* drops to 49.9 €/MWh compared to a rise in the *NPC* of the base case to 62.9 €/MWh. In Helsinki, the *NPC* ranges between 53.1 and 55.7 €/MWh, while its base case covers the heating demand at 51.5 €/MWh. These prices embody the CSHPSS plant in Helsinki as a competitive solution due to the high heating demand and high the non-renewable energy resources prices. By 2030, the *NPC* is expected to decrease below 46.7 €/MWh, while its base case continues to increase up to 62.7 €/MWh.

6. Conclusions

The EU ambitious plan to cut the GHG up to 40% simultaneously with increasing the share of the renewable energy resource at least 27% by 2030 encourages the prevalent methodology to quantify the renewable energy system's performance including its economic and environmental aspects. This work attempts to explore the prospects for wide-scale deployment of the central solar heating plants coupled with seasonal storage (CSHPSS) in the residential sector under various EU climate zones. The proposed methodological framework correspondingly based on a multi-objective approach which is applied to optimize the cost and the aggregated environmental metric throughout the life cycle of the CSHPSS system in comparison to conventional heating systems. In this context, the methodology is applied to various EU climates comprising Madrid, Athens, Berlin and Helsinki as representative for the Mediterranean, central European, and Nordic climates, respectively with consideration for the seasonal and short-term storage units and their respective load profiles based on the explored climate zones.

Following the life cycle assessment approach, the calculated optimal solutions demonstrate an environmental advancement for the CSHPSS plants at the considered EU climate zones in comparison to a heating system fueled by natural gas. The minimum impact solutions reduce the total environmental impact by 86.5%, 84.7%, 82.1%, and 82.9% for Madrid, Athens, Berlin, and Helsinki cases, respectively. While this improvement reaches only 42.9% for the climate zone of Athens at the minimum cost optimal solution due to the dependency on using natural gas as a competitive solution in comparison to the deployment of the solar energy equipment. On the other hand, the life cycle cost analysis shows a clear tendency for increasing the net present cost (*NPC*) under various EU climate zones compared to their base cases due to the high initial capital cost of CSHPSS plants. In the minimum cost solutions, the *NPC* raised by 1%, 33.3%, 16.9% and 3.12% for Madrid, Athens, Berlin, and Helsinki cases, respectively. This increment proofs the dependency of CSHPSS plants on the climate conditions, the heating demand, and the prices of non-renewable energy resources.

Furthermore, this raise relatively increases in the minimum impact solution, and it becomes more substantial in Athens, and Berlin since the *NPC* increases by 50.8%, and 25.3% for these cities respectively due to the low price of natural gas. Recalling the optimal solutions dependency on the design parameters, a detailed sensitivity analysis for the most relevant economic parameters in Madrid case study is presented. The sensitivity results aggravate a high dependency of the *NPC* of the plant on the natural gas price, the discount rate, the investment

cost, the operational cost, where decreasing these parameters by 20% contribute to a significant change in the *NPC* up to 10%. While the total environmental impact increases by 196% for the reduction of the natural gas price by 20%.

Following the challenges facing the CSHPSS in EU member states include high investment costs and the variation in the technical benefits. The proposed methodological framework successes in reducing this variation the system performance when introduced in various EU climate zones. Thus, the yearly solar fraction never goes below than 90.1% in the investigated climate zones where the ratio of seasonal storage tank volume to solar collector field area is around $8 \pm 0.5\,m^3/m^2$. From the economic point of view, the future development of the CSHPSS plant cost based on the historically observed learning curves combined with the clear tendency for the increment in the natural gas prices at various EU member states proposes a significant economic improvement in the competitiveness of the CSHPSS plant in comparison to the conventional system by 2020. However, the low heating demand and low prices of the natural gas and electricity in Athens (Mediterranean climate zone) provokes a limited improvement in the CSHPSS plant competitiveness until 2022.

In the real application of sizing community solar district heating network, the present framework can be beneficial for obtaining the right combination of design variables with maximizing its environmental impact incorporation with eliminating the oversizing system equipment. Furthermore, the proposed framework initiates a proportional optimal value regarding the seasonal storage tank and solar collector field of $8 \pm 0.5\,m^3/m^2$ which can serve as a guide for developing business models or establishing pilot storage plant.

Overall this study provides an effective tool for the techno-economic and environmental assessment of the CSHPSS at the residential sector which can be applied to plan its integration into the existing district heating fields. Furthermore, our study highlights the broad applicability of using CSHPSS in different EU climate as a sustainable alternative solution to the conventional systems based on natural gas. Even though in the real applications, such solar district heating systems are highly sensitive to the fluctuation in the fossil fuel prices and other economic parameters. Therefore, the competitiveness cannot be approved without clear and effective policies based on a longer-term view for the deployment of renewable energy systems in the EU with a goal of establishing a more sustainable energy infrastructure.

Acknowledgments

The authors would like to acknowledge financial support from the Spanish Ministry of Economy and Competitiveness (ENE2015-64117-C5-1-R (MINECO/FEDER), ENE2015-64117-C5-3-R (MINECO/FEDER) and CTQ2016-77968 (MINECO/FEDER)) and Martí i Franquès COFUND Fellowship program. This project has received funding from the European Union's Horizon 2020 research and innovation programme under the Marie Skłodowska-Curie grant agreement No. 713679. The authors at the University of Lleida would like to thank the Catalan Government for the quality accreditation given to their research group (2017 SGR 1537). GREA is certified agent TECNIO in the category of technology developers from the Government of Catalonia.

References

[1] Renewable Energy Policy Network for 21st Century (REN21). Renewables 2016-Global Status Report; 2016.
[2] U.S. Energy Information Administration. International Energy Outlook 2016; 2016. www.eia.gov/forecasts/ieo/pdf/0484(2016).pdf.
[3] Rezaie B, Rosen MA. District heating and cooling: review of technology and potential enhancements. Appl Energy 2012;93:2–10. https://doi.org/10.1016/j.apenergy.2011.04.020.
[4] British Petroleum. BP Statistical Review of World Energy 2017; 2017. http://www.bp.com/content/dam/bp/en/corporate/pdf/energy-economics/statistical-review-2017/bp-statistical-review-of-world-energy-2017-full-report.pdf.
[5] European Energy Agency. Final energy consumption by sector and fuel. Denmark; 2017. doi:CSI 027/ENER 016.
[6] Balaras CA, Gaglia AG, Georgopoulou E, Mirasgedis S, Sarafidis Y, Lalas DP. European residential buildings and empirical assessment of the Hellenic building stock, energy consumption, emissions and potential energy savings. Build Environ 2007;42:1298–314. https://doi.org/10.1016/j.buildenv.2005.11.001.
[7] EEA. Annual European Union greenhouse gas inventory 1990-2014 and inventory report 2016. Copenhagen; 2016.
[8] European Commission. Memo on the Renewable Energy and Climate Change Package. Brussels; 2008.
[9] European Commission. Communication from the commission to the European Parliament, the council, the European economic and social committee and the committee of the regions - a policy framework for climate and energy in the period from 2020 to 2030. Brussels; 2014.
[10] Olsthoorn D, Haghighat F, Mirzaei PA. Integration of storage and renewable energy into district heating systems: a review of modelling and optimization. Sol Energy 2016;136:49–64. https://doi.org/10.1016/j.solener.2016.06.054.
[11] Jamar A, Majid ZAA, Azmi WH, Norhafana M, Razak AA. A review of water heating system for solar energy applications. Int Commun Heat Mass Transf 2016;76:178–87. https://doi.org/10.1016/j.icheatmasstransfer.2016.05.028.
[12] Pinel P, Cruickshank CA, Beausoleil-Morrison I, Wills A. A review of available methods for seasonal storage of solar thermal energy in residential applications. Renew Sustain Energy Rev 2011;15:3341–59. https://doi.org/10.1016/j.rser.2011.04.013.
[13] Raluy R, Serra L, Guadalfajara M, Lozano M. Life cycle assessment of central solar heating plants with seasonal storage. Energy Proc 2014;48:966–76. https://doi.org/10.1016/j.egypro.2014.02.110.
[14] European Solar Thermal Industry Federation (ESTIF). Solar heat markets in Europe: Trends and Market Statistics 2016. Brussels; 2016.
[15] Carrilho da Graça G, Augusto A, Lerer MM. Solar powered net zero energy houses for southern Europe: feasibility study. Sol Energy 2012;86:634–46. https://doi.org/10.1016/j.solener.2011.11.008.
[16] Abokersh M, Osman M, El-Baz O, El-Morsi M, Sharaf O. Review on the use of phase change material in domestic solar water heating systems. Int J Energy Res 2018;42:329–57. https://doi.org/10.1002/er.3765.
[17] McDaniel B, Kosanovic D. Modeling of combined heat and power plant performance with seasonal thermal energy storage. J Energy Storage 2016;7:13–23. https://doi.org/10.1016/j.est.2016.04.006.
[18] Ibrahim NI, Al-Sulaiman FA, Rahman S, Yilbas BS, Sahin AZ. Heat transfer enhancement of phase change materials for thermal energy storage applications: a critical review. Renew Sustain Energy Rev 2017;74:26–50. https://doi.org/10.1016/j.rser.2017.01.169.
[19] Antoniadis CN, Martinopoulos G. Simulation of solar thermal systems with seasonal storage operation for residential scale applications. Proc Environ Sci 2017;38:405–12. https://doi.org/10.1016/j.proenv.2017.03.124.
[20] Dincer I. On thermal energy storage systems and applications in buildings. Energy Build 2002;34:377–88. https://doi.org/10.1016/S0378-7788(01)00126-8.
[21] Fisch M, Guigas M, Dalenbäck J. A review of large-scale solar heating systems in Europe. Sol Energy 1998;63:355–66. https://doi.org/10.1016/S0038-092X(98)00103-0.
[22] Hesaraki A, Holmberg S, Haghighat F. Seasonal thermal energy storage with heat pumps and low temperatures in building projects - a comparative review. Renew Sustain Energy Rev 2015;43:1199–213. https://doi.org/10.1016/j.rser.2014.12.002.
[23] Speyer E. Optimum storage of heat with a solar house. Sol Energy 1959;3:24–48. https://doi.org/10.1016/0038-092X(59)90004-0.
[24] Ochs F, Heidemann W, Müller-Steinhagen H. Performance of large-scale seasonal thermal energy stores. J Sol Energy Eng 2009;131:041005. https://doi.org/10.1115/1.3197842.
[25] Bankston CA. The status and potential of central solar heating plants with seasonal storage: an international Report. Adv. Sol. Energy. New York: Plenum Press; 1988. p. 352–444https://doi.org/10.1007/978-1-4613-9945-2_5.
[26] Tian Z, Perers B, Furbo S, Fan J. Annual measured and simulated thermal performance analysis of a hybrid solar district heating plant with flat plate collectors and parabolic trough collectors in series. Appl Energy 2017;205:417–27. https://doi.org/10.1016/j.apenergy.2017.07.139.
[27] Weiss W, Spörk-Dür M, Mauthner F. Solar heat worldwide: global market development and trends in 2016. Austria: Gleisdorf; 2017.
[28] European Solar Thermal Industry Federation. Solar Thermal Markets in Europe. Trends and Market Statistics 2014. Brussel – Belgium; 2015.
[29] Schultz J, Andersen E, Furbo S. Advanced storage concepts for solar and low energy buildings, IEA-SHC Task 32. Copenhagen; 2008.
[30] Xu J, Wang RZ, Li Y. A review of available technologies for seasonal thermal energy storage. Sol Energy 2014;103:610–38. https://doi.org/10.1016/j.solener.2013.06.006.
[31] Rad FM, Fung AS. Solar community heating and cooling system with borehole thermal energy storage - review of systems. Renew Sustain Energy Rev 2016;60:1550–61. https://doi.org/10.1016/j.rser.2016.03.025.
[32] Shah SK, Aye L, Rismanchi B. Seasonal thermal energy storage system for cold climate zones: a review of recent developments. Renew Sustain Energy Rev 2018;97:38–49. https://doi.org/10.1016/j.rser.2018.08.025.
[33] Sibbitt B, McClenahan D, Djebbar R, Thornton J, Wong B, Carriere J, et al. The performance of a high solar fraction seasonal storage district heating system - five years of operation. Energy Proc 2012;30:856–65. https://doi.org/10.1016/j.egypro.2012.11.097.
[34] Rehman Hur, Hirvonen J, Sirén K. A long-term performance analysis of three different configurations for community-sized solar heating systems in high

latitudes. Renew Energy 2017;113:479–93. https://doi.org/10.1016/j.renene.2017.06.017.
[35] Rämä M, Mohammadi S. Comparison of distributed and centralised integration of solar heat in a district heating system. Energy 2017;137:649–60. https://doi.org/10.1016/j.energy.2017.03.115.
[36] Rad FM, Fung AS, Rosen MA. An integrated model for designing a solar community heating system with borehole thermal storage. Energy Sustain Dev 2017;36:6–15. https://doi.org/10.1016/j.esd.2016.10.003.
[37] Panno D, Buscemi A, Beccali M, Chiaruzzi C, Cipriani G, Ciulla G, et al. A solar assisted seasonal borehole thermal energy system for a non-residential building in the Mediterranean area. Sol Energy 2018. https://doi.org/10.1016/j.solener.2018.06.014.
[38] Ciampi G, Rosato A, Sibilio S. Thermo-economic sensitivity analysis by dynamic simulations of a small Italian solar district heating system with a seasonal borehole thermal energy storage. Energy 2018;143:757–71. https://doi.org/10.1016/j.energy.2017.11.029.
[39] Li X, Liu M, Duanmu L, Ji Y. The optimization of solar heating system with seasonal storage based on a real project. Proc Eng 2015;121:1341–8. https://doi.org/10.1016/j.proeng.2015.09.017.
[40] Durão B, Joyce A, Mendes JF. Optimization of a seasonal storage solar system using Genetic Algorithms. Sol Energy 2014;101:160–6. https://doi.org/10.1016/j.solener.2013.12.031.
[41] Rehman Hur, Hirvonen J, Sirén K. Influence of technical failures on the performance of an optimized community-size solar heating system in Nordic conditions. J Clean Prod 2018;175:624–40. https://doi.org/10.1016/j.jclepro.2017.12.088.
[42] Hirvonen Jur, Rehman H, Sirén K. Techno-economic optimization and analysis of a high latitude solar district heating system with seasonal storage, considering different community sizes. Sol Energy 2018;162:472–88. https://doi.org/10.1016/j.solener.2018.01.052.
[43] Buoro D, Pinamonti P, Reini M. Optimization of a distributed cogeneration system with solar district heating. Appl Energy 2014;124:298–308. https://doi.org/10.1016/j.apenergy.2014.02.062.
[44] Tulus V, Boer D, Cabeza LF, Jiménez L, Guillén-Gosálbez G. Enhanced thermal energy supply via central solar heating plants with seasonal storage: a multi-objective optimization approach. Appl Energy 2016;181:549–61. https://doi.org/10.1016/j.apenergy.2016.08.037.
[45] Pavičević M, Novosel T, Pukšec T, Duić N. Hourly optimization and sizing of district heating systems considering building refurbishment – case study for the city of Zagreb. Energy 2017;137:1264–76. https://doi.org/10.1016/j.energy.2017.06.105.
[46] Welsch B, Göllner-Völker L, Schulte DO, Bär K, Sass I, Schebek L. Environmental and economic assessment of borehole thermal energy storage in district heating systems. Appl Energy 2018;216:73–90. https://doi.org/10.1016/j.apenergy.2018.02.011.
[47] Paiho S, Hoang H, Hukkalainen M. Energy and emission analyses of solar assisted local energy solutions with seasonal heat storage in a Finnish case district. Renew Energy 2017;107:147–55. https://doi.org/10.1016/j.renene.2017.02.003.
[48] Flynn C, Sirén K. Influence of location and design on the performance of a solar district heating system equipped with borehole seasonal storage. Renew Energy 2015;81:377–88. https://doi.org/10.1016/j.renene.2015.03.036.
[49] Edenhofer O, Pichs-Madruga R, Sokona Y, Seyboth K, Eickemeier P, Matschoss P, et al. Renewable energy sources and climate change mitigation: summary for policymakers and technical summary; 2011 https://doi.org/10.5860/CHOICE.49-6309.
[50] Bauer D, Marx R, Drück H. Solar district heating for the built environment technology and future trends within the european project Einstein. Energy Proc 2014;57:2716–24. https://doi.org/10.1016/j.egypro.2014.10.303.
[51] Teske S, Janis L, Luis C, Marcel B, Elena D, Christoph R. Solar thermal electricity global outlook 2016. Amsterdam; 2016. https://doi.org/10.4321/S2254-28842015000200009.
[52] Carpaneto E, Lazzeroni P, Repetto M. Optimal integration of solar energy in a district heating network. Renew Energy 2015;75:714–21. https://doi.org/10.1016/j.renene.2014.10.055.
[53] ur Rehman Hassam, Hirvonen Janne, Sirén Kai. Performance comparison between optimized design of a centralized and semi-decentralized community size solar district heating system. Appl Energy 2018;229:1072–94. https://doi.org/10.1016/j.apenergy.2018.08.064.
[54] lein SA, et al. TRNSYS 18: a transient system simulation program. Madison, USA: Solar Energy Laboratory, University of Wisconsin; 2017. http://sel.me.wisc.edu/trnsys.
[55] GenOpt Wetter M. Generic Optimization Program. User Manual. Berkeley Lab; 2016. p. 1–108.
[56] Bauer D, Marx R, Nußbicker-Lux J. German central solar heating plants with seasonal heat storage. Sol Energy 2010;84:612–23. https://doi.org/10.1016/j.solener.2009.05.013.
[57] Raab S, Mangold D, Müller-Steinhagen H. Validation of a computer model for solar assisted district heating systems with seasonal hot water heat store. Sol Energy 2005;79:531–43. https://doi.org/10.1016/j.solener.2004.10.014.
[58] Gebreslassie B, Guillén-Gosálbez G. Design of environmentally conscious absorption cooling systems via multi-objective optimization and life cycle assessment. Appl Energy 2009;86:1712–22. https://doi.org/10.1016/j.apenergy.2008.11.019.
[59] Sameti M, Haghighat F. A two-level multi-objective optimization for simultaneous design and scheduling of a district energy system. Appl Energy 2017;208:1053–70. https://doi.org/10.1016/j.apenergy.2017.09.046.
[60] Di Somma M, Yan B, Bianco N, Graditi G, Luh PB, Mongibello L, et al. Multi-objective design optimization of distributed energy systems through cost and exergy assessments. Appl Energy 2017;204:1299–316. https://doi.org/10.1016/j.apenergy.2017.03.105.
[61] Guadalfajara M, Lozano MA, Serra LM. Evaluation of the potential of large solar heating plants in Spain. Energy Proc 2012;30:839–48. https://doi.org/10.1016/j.egypro.2012.11.095.
[62] Duffie JA, Beckman WA, Solar Worek WM. Engineering of thermal processes. J Sol Energy Eng 1994;116:67. https://doi.org/10.1115/1.2930068.
[63] Allouhi A, Agrouaz Y, Benzakour Amine M, Rehman S, Buker MS, Kousksou T, et al. Design optimization of a multi-temperature solar thermal heating system for an industrial process. Appl Energy 2017;206:382–92. https://doi.org/10.1016/j.apenergy.2017.08.196.
[64] Hobbi A, Siddiqui K. Optimal design of a forced circulation solar water heating system for a residential unit in cold climate using TRNSYS. Sol Energy 2009;83:700–14. https://doi.org/10.1016/j.solener.2008.10.018.
[65] Hang Y, Qu M, Ukkusuri S. Optimizing the design of a solar cooling system using central composite design techniques. Energy Build 2011;43:988–94. https://doi.org/10.1016/j.enbuild.2010.12.024.
[66] Kalogirou SA. Solar energy engineering: processes and systems. 1st ed. Academic Press; 2009https://doi.org/10.1016/B978-0-12-374501-9.00014-5.
[67] Gluch P, Baumann H. The life cycle costing (LCC) approach: a conceptual discussion of its usefulness for environmental decision-making. Build Environ 2004;39:571–80. https://doi.org/10.1016/j.buildenv.2003.10.008.
[68] Chemical Engineering Plant Cost Index (CEPCI): Economic Indicator. Chem Eng J; 2015. http://www.chemengonline.com/pci-home [accessed July 13, 2015].
[69] Turton R, Bailie RC, Whiting WB, Shaeiwitz JA, Bhattacharyya D. Analysis, synthesis, and design of chemical processes. 3rd ed. Prentice Hall; 2008.
[70] Ellehauge K, Pedersen TE. Solar heat storages in district heating networks. Energinet.dk, PREHEAT project no. 2006-2-6750; 2007.
[71] Schmidt T, Mangold D. Status of solar thermal seasonal storage in Germany. Effstock; 2009.
[72] Calise F, Dentice d'Accadia M, Palombo A. Transient analysis and energy optimization of solar heating and cooling systems in various configurations. Sol Energy 2010;84:432–49. https://doi.org/10.1016/j.solener.2010.01.001.
[73] Nemerow NL, Agardy FJ, Sullivan P, Salvato JA. Environmental engineering: environmental health and safety for municipal infrastructure, land use and planning, and industry. 6th ed. John Wiley & Sons, Inc; 2009.
[74] ISO/TC 207/SC 5. ISO 14040:2006 Environmental management — Life cycle assessment — Principles and framework; 2006.
[75] International Organization for Standardization (ISO). ISO 14041: Environmental Management - Life Cycle Assessment: Goal and Scope Definition and Inventory Analysis; 1997.
[76] International Organization for Standardization (ISO). ISO 14042:Environmental management - Life cycle assessment - Life cycle impact; 2000.
[77] Guillén-Gosálbez G, Caballero JA, Jiménez L. Application of life cycle assessment to the structural optimization of process flowsheets. Ind Eng Chem Res 2008;47:777–89. https://doi.org/10.1016/S1570-7946(07)80218-5.
[78] Weidema BP, Bauer C, Hischier R, Mutel C, Nemecek T, Reinhard J, et al. Data quality guideline for the ecoinvent database version 3. vol. 3; 2013.
[79] Goedkoop M, Heijungs R, De Schryver A, Struijs J, van Zelm R. ReCiPe 2008. A LCIA method which comprises harmonised category indicators at the midpoint and the endpoint level. Report I: Characterisation; 2009. p. 1–133. http://www.lcia-recipe.net.
[80] JRC European commission (JRC-IES). ILCD Handbook: Recommendations for Life Cycle Impact Assessment in the European context. 1st ed. Luxemburg: Office of the European Union; 2011. https://doi.org/10.278/33030.
[81] Weiss W, Biermayr P. Potential of Solar Thermal in Europe; 2010.
[82] Paul Hutchens. Solar Heating Roadmap: Strategy and Measures of the Solar Heating Industry for Accelerated Market Growth to 2030. Berlin; 2012.
[83] Greenpeace international. Energy Revolution: A sustainable pathway to a clean energy future for Europe; 2005.
[84] Rout UK, Blesl M, Fahl U, Remme U, Voß A. Uncertainty in the learning rates of energy technologies: an experiment in a global multi-regional energy system model. Energy Policy 2009;37:4927–42. https://doi.org/10.1016/j.enpol.2009.06.056.
[85] Rubin ES, Azevedo IML, Jaramillo P, Yeh S. A review of learning rates for electricity supply technologies. Energy Policy 2015;86:198–218. https://doi.org/10.1016/j.enpol.2015.06.011.
[86] Vecchietti A, Lee S, Grossmann IE. Modeling of discrete/continuous optimization problems: characterization and formulation of disjunctions and their relaxations. Comput Chem Eng 2003;27:433–48. https://doi.org/10.1016/S0098-1354(02)00220-X.
[87] Ehrgott M. Multicriteria optimization. Heidelberg: Springer; 2005.
[88] Kennedy J, Eberhart R. Particle swarm optimization. Neural networks. In: 1995 Proceedings, IEEE Int Conf, vol. 4; 1995. p. 1942–8. https://doi.org/10.1109/ICNN.1995.488968.
[89] Kennedy J, Eberhart RC. A discrete binary version of the particle swarm algorithm. 1997 IEEE Int Conf Syst Man, Cybern Comput Cybern Simul. 1997. p. 4–8https://doi.org/10.1109/ICSMC.1997.637339.
[90] Hooke R, Jeeves TA. "Direct Search" solution of numerical and statistical problems. J ACM 1961;8:212–29. https://doi.org/10.1145/321062.321069.
[91] IDAE. Análisis del consumo energético del sector residencial en España. INFORME FINAL; 2011.
[92] Shariah A, Al-Akhras MA, Al-Omari IA. Optimizing the tilt angle of solar collectors. Renew Energy 2002;26:587–98. https://doi.org/10.1016/S0960-1481(01)00106-9.
[93] United Nations Environment Programme, Solar Thermal Energy Technology Fact

Sheet; 2014.
[94] Colclough S, McGrath T. Net energy analysis of a solar combi system with Seasonal Thermal Energy Store. Appl Energy 2015;147:611–6. https://doi.org/10.1016/j.apenergy.2015.02.088.
[95] Kottek M, Grieser J, Beck C, Rudolf B, Rubel F. World map of the Köppen-Geiger climate classification updated. Meteorol Zeitschrift 2006;15:259–63. https://doi.org/10.1127/0941-2948/2006/0130.
[96] Rubel F, Kottek M. Observed and projected climate shifts 1901–2100 depicted by world maps of the Köppen-Geiger climate classification. Meteorol Zeitschrift 2010;19:135–41. https://doi.org/10.1127/0941-2948/2010/0430.
[97] U.S. Department of Energy. EnergyPlus. Energy Simulation Software: Weather Data n.d. http://apps1.eere.energy.gov/buildings/energyplus/ [accessed March 23, 2018].
[98] European Commission. Eurostat. Energy database n.d. http://ec.europa.eu/eurostat/data/database [accessed May 10, 2018].
[99] Weidema BP, Bauer C, Hischier R, Mutel C, Nemecek T, Reinhard J, et al. The ecoinvent database: overview and methodology, Data quality guideline for the ecoinvent database version 3; 2013. www.ecoinvent.org.
[100] Trimble. SketchUp 2017. http://www.sketchup.com.
[101] Ahmed K, Pylsy P, Kurnitski J. Hourly consumption profiles of domestic hot water for different occupant groups in dwellings. Sol Energy 2016;137:516–30. https://doi.org/10.1016/j.solener.2016.08.033.
[102] Instituto de Estadística. Trends in households in the European Union: 1995–2025; 2003.
[103] Parakosta K, Papageorgiou N, Sotiropoulos B. Residential hot water use pattern in Greece. Sol Energy 1995;54:369–74.
[104] Ahmed K, Pylsy P, Kurnitski J. Monthly domestic hot water profiles for energy calculation in Finnish apartment buildings. Energy Build 2015;97:77–85. https://doi.org/10.1016/j.enbuild.2015.03.051.
[105] Jordan U, Vajen K. DHWcalc: program to generate domestic hot water profiles with statistical means for user defined conditions. In: Proc. ISES Sol. World Congr., Orlando (US): n.d. p. 8–12.
[106] Eurostat. Inflation in the euro area 2018. https://ec.europa.eu/eurostat/.../Inflation_in_the_euro_area [accessed March 12, 2018].
[107] Braungardt S, Eichhammer W, Elsland R, Fleiter T, Klobasa M, Krail M, et al. Study evaluating the current energy efficiency policy framework in the EU and providing orientation on policy options for realising the cost-effective energy-efficiency/saving potential until 2020 and beyond. Karlsruhe/Vienna/Rome; 2014.
[108] Greenpeace international. Energy [R]evolution - A sustainable EU 27 energy outlook; 2012.
[109] Joachim Nitsch, Thomas Pregger, Scholz Y, Naegler T, Sterner M, Gerhardt N, et al. Langfristszenarien und Strategien für den Ausbau der Erneuerbaren Energien in Deutschland bei Berücksichtigung der Entwicklung in Europa und global; 2012. doi:BMU - FKZ 03MAP146.
[110] Kost C, Mayer JN, Thomsen J, Hartmann N, Senkpiel C, Philipps S, et al. Levelized cost of electricity renewable energy technologies. Freiburg, Germany; 2013. https://10.1613/jair.301.
[111] Montgomery DC. Design and analysis of experiments. eighth ed. John Wiley & Sons, Inc.; 2013.